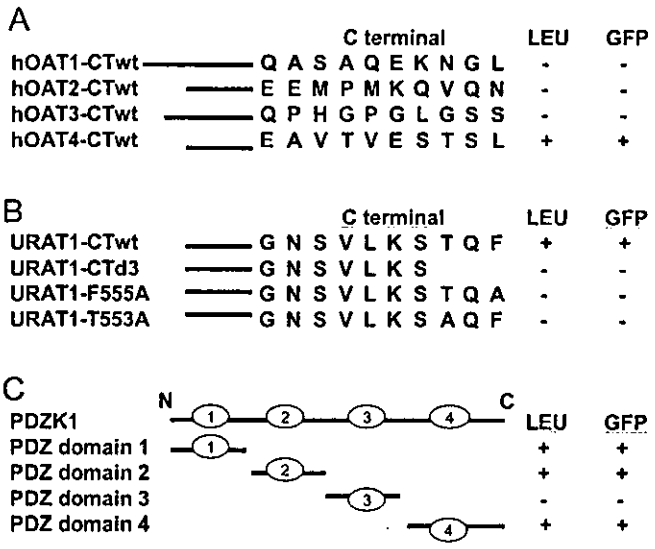

FIG. 1. **Specificity of PDZK1 for interaction with C terminus of URAT1 in the yeast two-hybrid system.** *A*, full-length PDZK1 interacting with the intracellular C terminus of OAT4 but not C termini of other OATs. *B*, PDZK1 specifically interacted with C-terminal wild-type URAT1 but not with the C-terminal URAT1 mutants F555A, T553A, and d3 (553–555). *C*, the URAT1 C-terminal wild-type bait interacts with the prey containing the first, second, or fourth PDZ domain of PDZK1. The specificity of the prey containing a single PDZ domain of PDZK1 for the URAT1 bait was further confirmed by the absence of growth associated with the URAT1 d3 mutant baits. The *bars* represent the approximate length of the baits, and the sequence of the last 10 amino acids is shown. The pJG4-5 cDNA library expression cassette is under the control of the GAL1 promoter, such that library proteins are expressed in the presence of galactose but not glucose. The system used for the two-hybrid screen includes the reporter genes LEU2 and GFP, which replace the commonly used *lacZ* gene; it allows a fast and easy detection of positive clones with long-wave length UV. The results of growth assay and GFP fluorescence monitoring are shown on the *right*.

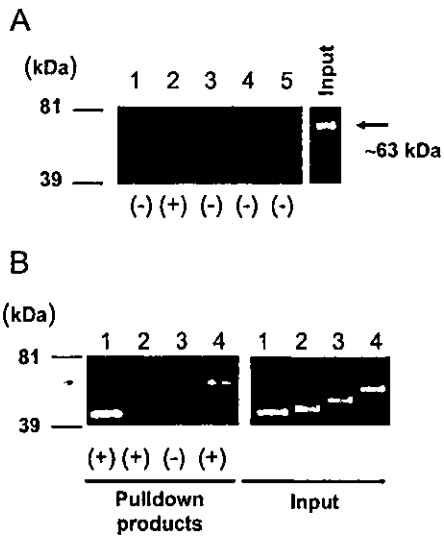

FIG. 2. **Interaction between PDZK1 and the C terminus of URAT1.** *A*, the GST protein fused to C-terminal wild-type URAT1 can coprecipitate PDZK1, confirming the specificity found in the yeast two-hybrid system. The mutant form of URAT1 in which the C-terminal PDZ recognition motif is removed cannot precipitate PDZK1. The full-length PDZK1 PCR product was *in vitro*-translated in the presence of Transcend biotinylated lysine tRNA (Promega). The *in vitro* translation products were incubated with GST alone (*lane 1*), GST-URAT1-CT-wt (*lane 2*), GST-URAT1-CT-d3 (*lane 3*), GST-URAT1-CT-F555A (*lane 4*), or GST-URAT1-CT-T553A (*lane 5*) using the ProFound Pull-Down GST Protein:Protein Interaction kit (Pierce). The pull-down products were analyzed by SDS-PAGE. The input corresponds to the crude *in vitro* translation reaction. The positions of molecular mass standards are shown on the *right*. *B*, domain analysis of PDZK1 individual PDZ domains. The GST-URAT1-CT-wt bound columns were incubated with MagExtracter (TOYOBO)-purified MBP-fused proteins containing single, one-PDZ domain, PDZ1 (*lane 1*), PDZ2 (*lane 2*), PDZ3 (*lane 3*), and PDZ4 (*lane 4*) of PDZK1. The expressed fusion proteins were detected with anti-MBP antiserum (New England Biolabs).

PDZ domains of PDZK1, we produced prey vectors each containing individual PDZ domain (PDZ1, PDZ2, PDZ3, and PDZ4). The interaction with URAT1 C terminus was observed for PDZ1, PDZ2, and PDZ4 but not for PDZ3 of PDZK1 (Fig. 1*C*).

In Vitro Binding of URAT1 and PDZK1—To confirm *in vitro* the ability of the C terminus of URAT1 to bind with PDZK1, we used GST pull-down assay to validate the protein-protein interaction (Fig. 2*A*). GST fusion proteins bearing the wild-type C-terminal region (URAT1-CT-wt) or C-terminal region mutants (URAT1-CT-d3, F555A, and T553A) of URAT1 were used to pull down the full-length PDZK1 from *in vitro* translation experiments. The data showed the same specificity of the interaction of PDZK1 and URAT1 as exhibited in the yeast two-hybrid assays (Fig. 1*B*). As expected, we did not observe the binding of PDZK1 to the URAT1 in which the C-terminal PDZ recognition motif was removed (URAT1-CT-d3) or mutated (URAT1-CT-F555A or URAT1-CT-T553A) (Fig. 2*A*).

To confirm the binding specificity between URAT1 C terminus and PDZK1 PDZ domains, we generated MBP-fused proteins consisting of PDZK1 individual PDZ domain (PDZ1, PDZ2, PDZ3, or PDZ4) and tested the interaction with GST-fused URAT1-CT-wt. Fig. 2*B* shows that MBP-PDZ1, MBP-PDZ2, and MBP-PDZ4 could bind with URAT1 C terminus same as the results obtained from the yeast two-hybrid assays (Fig. 1*C*).

These interaction specificities were further confirmed by surface plasmon resonance (SPR) method. We observed dose-responsive bindings of the PDZ1, PDZ2, and PDZ4 domains of PDZK1 fused with MBP to an immobilized URAT1 C terminus (Fig. 3, *A*, *B*, and *D*). In contrast, no significant binding was detected in the PDZ3 domain of PDZK1 (Fig. 3*C*). The results of kinetic analysis performed on all four single PDZ domains of PDZK1 are summarized in Table I. The dissociation constant (K_D) values are as follows: PDZK1 PDZ1 domain, 1.97 nM; PDZ2 domain, 514 nM; and PDZ4 domain, 296 nM for URAT1 C terminus. These binding affinities are similar to the value reported for the interaction between CAP70 and CFTR (K_D = 8–220 nM) (14).

Coimmunoprecipitation of URAT1 and PDZK1 from Heterologous Cells and from Human Kidney Membrane Fraction—To demonstrate that URAT1 and PDZK1 can also interact in mammalian cells, first we generated a rabbit anti-PDZK1 polyclonal antibody directed against the N-terminal 14 amino acids of human PDZK1. This antibody was tested by Western blot analysis using human normal adult kidney protein extracts and crude membrane fractions from HEK293 cells transfected with pcDNA3.1-PDZK1. Western blot analysis showed that the anti-PDZK1 antibody reacted with a strong band of ~63-kDa is consistent with PDZK1 on a human kidney protein extract and with a strong band of ~70-kDa and a weak band of ~63-kDa on crude membrane fractions from PDZK1-transfected HEK293 cells (Fig. 4*A*). Because the weak 63-kDa band was also identified in cells transfected with vector alone (pcDNA3.1) and we detected the PDZK1 mRNA expression in HEK293 cells by RT-PCR (data not shown), these weak bands may be explained by the endogenous expression of PDZK1 in these cells rather than an artifact. All of these bands disappeared after the incubation of synthetic peptides (200 μg/ml, data not shown). The different molecular sizes detected in the kidney and in HEK293 cells may be due to the different post-translational modification in the native tissues and the cells.

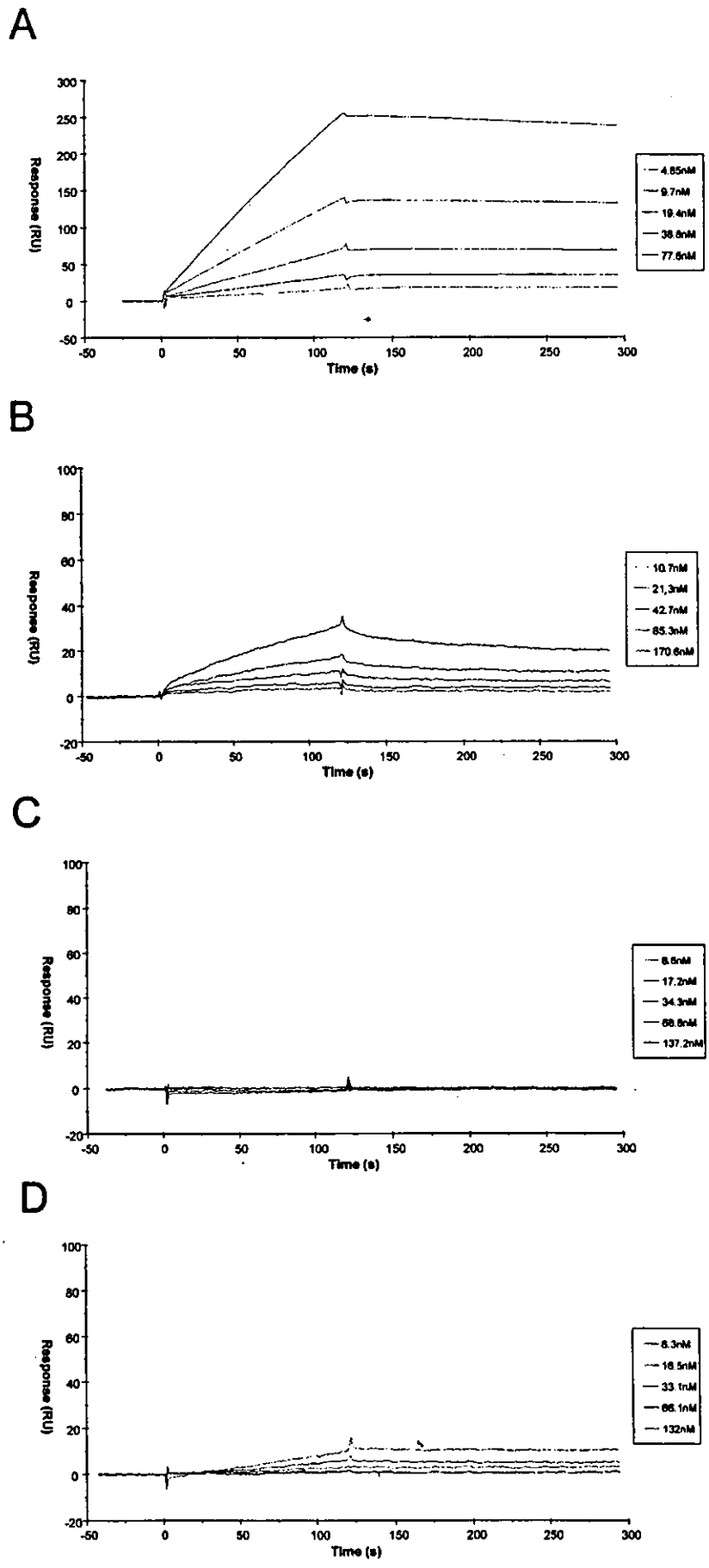

FIG. 3. **Surface plasmon resonance analyses of the interaction between C terminus of URAT1 and the PDZK1 single PDZ domains.** *A*, the binding of the PDZK1 PDZ domain 1 fused with MBP, at different concentrations, to the URAT1 C terminus. *B*, the binding of the PDZK1 PDZ domain 2 fused with MBP, at different concentrations, to the URAT1 C terminus. *C*, the binding of the PDZK1 PDZ domain 3 fused with MBP, at different concentrations, to the URAT1 C terminus. *D*, the binding of the PDZK1 PDZ domain 4 fused with MBP, at different concentrations, to the URAT1 C terminus.

TABLE I
Characteristics of the interaction between PDZK1 individual PDZ domains and URAT1 C terminus

The kinetic characteristics of the interaction with immobilized GST-fused URAT1 C terminus with single one-PDZ domains of PDZK1 (PDZ1–4) fused with MBP are summarized (see Fig. 3). Association rate constants (k_a), dissociation rate constants (k_d), and equilibrium dissociation constants ($K_D = k_d/k_a$) are given.

Construct	k_a	k_d	K_D
	1/mM·s	*1/min*	*nM*
PDZK1-PDZ1	3.45×10^5	6.79×10^{-4}	1.97
PDZK1-PDZ2	4.02×10^3	2.07×10^{-3}	514
PDZK1-PDZ3	—[a]	—	No binding
PDZK1-PDZ4	1.89×10^3	5.61×10^{-4}	296

[a] —, not binding detectable.

FIG. 4. **Coimmunoprecipitation of URAT1 and PDZK1 proteins in HEK293 cell lysates and from human kidney membrane fractions.** *A*, Western blot analysis of normal human kidney protein extract (*lane 1*), and crude membranes from HEK293 transfected with PDZK1 (*lane 2*) and from HEK293 transfected with mock (*lane 3*). A single strong band of ~63 kDa, which is consistent with PDZK1, was observed in *lane 1*, a strong band of ~70 kDa and a weak band of 63 kDa were observed in *lane 2*, and a weak band of 63 kDa was observed in *lane 3*. *B*, HEK293 cells were transfected with pEGFP-C2 vectors alone (*lane 1*) or vectors encoding wild-type URAT1 (*lane 2*) or URAT1-d3 (*lane 3*) with pcDNA3.1-PDZK1 and coimmunoprecipitated with the anti-GFP antibody. Then, the coimmunoprecipitates were resolved by SDS-PAGE and probed with anti-PDZK1 antibodies. *C*, human kidney membrane fractions were immunoprecipitated with control IgG and anti-PDZK1 antibody. The presence of URAT1 in the immunoprecipitates was determined by Western blotting with the anti-URAT1 C-terminal antibody used in previous report (4).

Then, we expressed pEGFP-C2 vector alone and coexpressed GFP-fused full-length human URAT1 wt and d3 with PDZK1 in HEK293 cells. Wild-type EGFP-URAT1 was coimmunoprecipitated with a GFP-specific antibody with a strong 70-kDa band (and a very faint 63-kDa band after long exposure), but EGFP-URAT1 lacking the last three amino acids and vector alone was not (Fig. 4*B*). These results also confirm the interaction between PDZK1 and URAT1 detected in the yeast two-hybrid system, in addition to other *in vitro* binding assays.

Furthermore, we demonstrated an association between endogenous PDZK1 and URAT1 in tissue by coimmunoprecipitating URAT1 from human kidney membrane fractions using PDZK1 antibody, but not control IgG (Fig. 4*C*). This result provided us evidence that the observed interaction occurs between protein partners expressed from the endogenous genes in relevant tissue.

Tissue Distribution of URAT1 and PDZK1 mRNA in Human Tissues—In humans, URAT1 has been detected exclusively in the kidney (4), and PDZK1 has been detected mainly in the liver, kidney, pancreas, gastrointestinal tract, and adrenal cortex (19), but their expressions in other tissues has not yet been analyzed. Using human multiple-cDNA panels, we examined the mRNA distributions of both URAT1 and PDZK1. The URAT1 transcript was detected strongly in the kidney, whereas the PDZK1 transcripts were detected in most of the tissues analyzed in a various levels of intensity, confirming and expanding the previously described distribution in humans (Fig. 5*A*).

Coexpression of URAT1 and PDZK1 in the Human Kidney—URAT1 is present at the luminal (apical) membrane of proximal tubules (4), and PDZK1 is reported to be expressed at the brush border (apical) of the proximal tubular cells (19). To determine whether URAT1 and PDZK1 colocalize at the apical membrane of the renal proximal tubules, we performed immunostaining of serial kidney sections with the anti-URAT1 and anti-PDZK1 antibodies. Consistent with the previous reports, in the renal cortex, the overlapping expressions of URAT1 and PDZK1 was detected in most of the proximal tubular cells (Fig. 5, *B* and *C*). The specificities of each antibody were confirmed by the reduced immunoreactivities caused by the preincubation of the antibodies with the corresponding synthetic peptides (200 μg/ml, data not shown).

URAT1 Transport Activity Increases in the Presence of PDZK1—To determine whether URAT1/PDZK1 interactions change URAT1 activity, we transfected transiently HEK293 cells with the pcDNA3.1(+) construct containing full-length URAT1 or URAT1 lacking the last three amino acids of its C-terminal. At an incubation time of 1 min, we demonstrated that the uptake of [^{14}C]urate by the wild-type URAT1 and URAT1 deletion mutant were from 3- to 4-fold higher than that by the mock (Fig. 6*A*). When full-length URAT1 coexpressed with pcDNA3.1(+) containing PDZK1, the coexpression significantly increased urate transport activity by 1.4-fold (Fig. 6*A*). This effect was abolished when the C-terminal deletion mutant of URAT1 (URAT1-d3) was coexpressed with PDZK1. These results indicate that an interaction between the URAT1 C terminus and PDZK1 is necessary for the functional increase of urate transport.

Next, we examined the effect of PDZK1 on the kinetics of [^{14}C]urate transport via URAT1 stably expressed in HEK293 cells (HEK-URAT1) that had been transfected with pcDNA3.1-PDZK1 or vector (pcDNA3.1) alone. Kinetic data showed that PDZK1 increased the V_{max} significantly ($p < 0.05$) from 2.78 ± 0. 34 to 3.34 ± 0.25 nanomoles/mg of protein/min but did not change the K_m (from 203.8 ± 25.6 to 198.7 ± 33.3 μM) ($p = 0.78$) (Fig. 6*B*).

To determine changes in the cell surface expression level of URAT1, we used a cell membrane-impermeant biotinylation reagent to label cell surface proteins selectively. After the treatment, cell lysates from HEK-URAT1 cells transfected with pcDNA3.1-PDZK1 or pcDNA3.1 alone were collected. The amount of surface-biotinylated URAT1 expression on plasma membranes increased 2.1-fold (mock-transfected: 29.0 ± 3.66 *versus* PDZK1-transfected: 60.1 ± 18.9 arbitrary units, $n = 3$) when PDZK1 was coexpressed (Fig. 6, *C* and *D*). This change seems close to the one in V_{max} of URAT1-mediated transport observed in Fig. 6*B*.

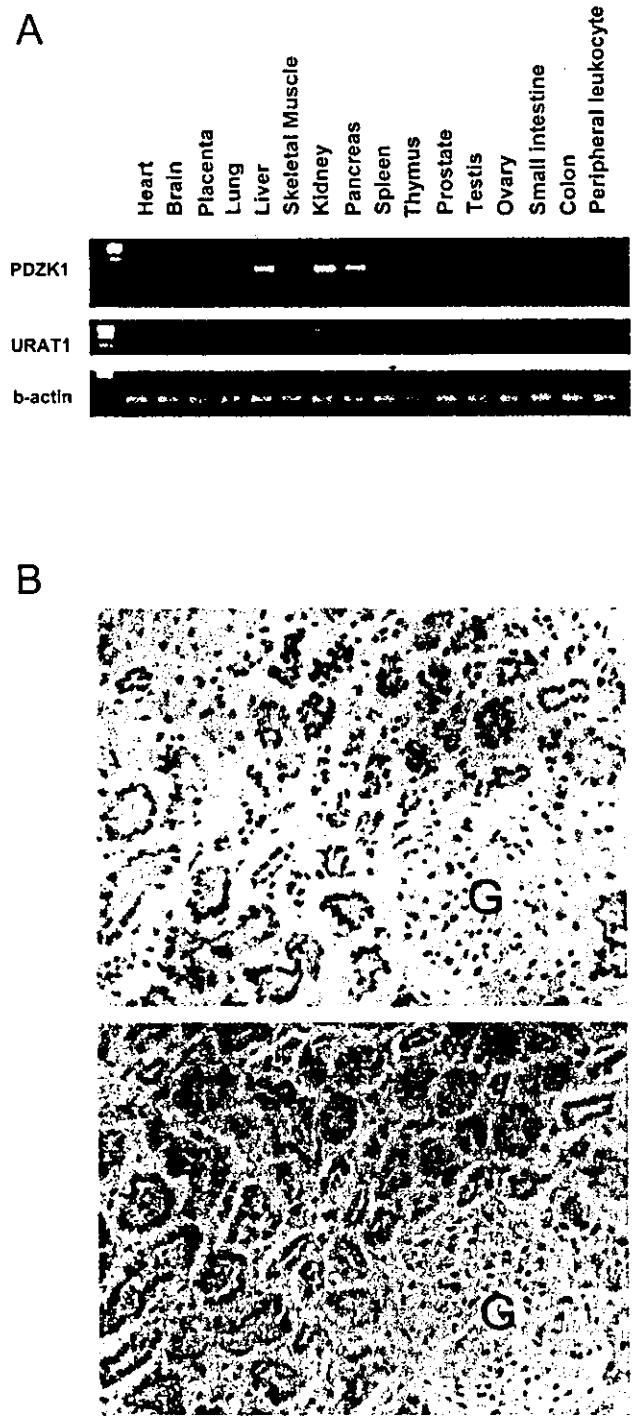

FIG. 5. **Colocalization of URAT1 and PDZK1.** *A*, distributions of URAT1 and PDZK1 mRNA in human multiple cDNA panels. URAT1 and PDZK1 expression overlaps in kidney, which is the sole site of URAT1 expression. Control amplification with β-actin was performed in parallel (*bottom panel*). *B*, immunohistochemical analysis of URAT1 and PDZK1 in serial sections of human kidney. URAT1 was detected in the apical membrane of renal proximal tubules (*upper panel*) and no staining was observed in the basolateral membrane and glomeruli (*G*). PDZK1 was also detected in the apical membrane of proximal tubules (*lower panel*).

DISCUSSION

URAT1 is of primary importance in regulating blood urate level in humans. Through a yeast two-hybrid screen of a human kidney cDNA library, we identified PDZK1 as a binding partner of URAT1. PDZK1 is a PDZ domain-containing protein that was originally identified as a protein that interacts with MAP17, a membrane-associated protein (19). In addition to MAP17, PDZK1 has also been reported to interact with several membrane proteins through its PDZ domain; these proteins include the type IIa Na/P_i cotransporter (26), scavenger receptor class B type I (SR-BI) (27), CFTR (14), and multidrug resistance-associated protein MRP2 (cMOAT) (28).

Here we report the specific interaction between URAT1 and PDZK1 as demonstrated by yeast two-hybrid assays, pull-down assays, surface plasmon resonance (SPR) analysis, coimmunoprecipitation, and colocalization experiments. The C-terminal of URAT1 (STQF) falls into class I ((S/T)XØ, where Ø indicates a hydrophobic residue) of the PDZ-binding motif (9, 10). All the proteins that interact with PDZK1 except SR-BI (EAKL, class II) (27) have the PDZ-binding motif belonging to class I; type IIa Na/Pi, ATRL (26): CFTR, DTRL (14): and MRP2, STKF (28). The results obtained using the various mutants of the URAT1 C-terminal in yeast two-hybrid and GST pull-down assays (Figs. 1 and 2) confirmed the importance of the 0 and −2 positions of the PDZ motif (9, 10). Furthermore, the interaction profiles of the C termini of the PDZK1 partner against each PDZ domain of PDZK1, which were confirmed by GST pull-down assay and SPR analysis, were different, although they

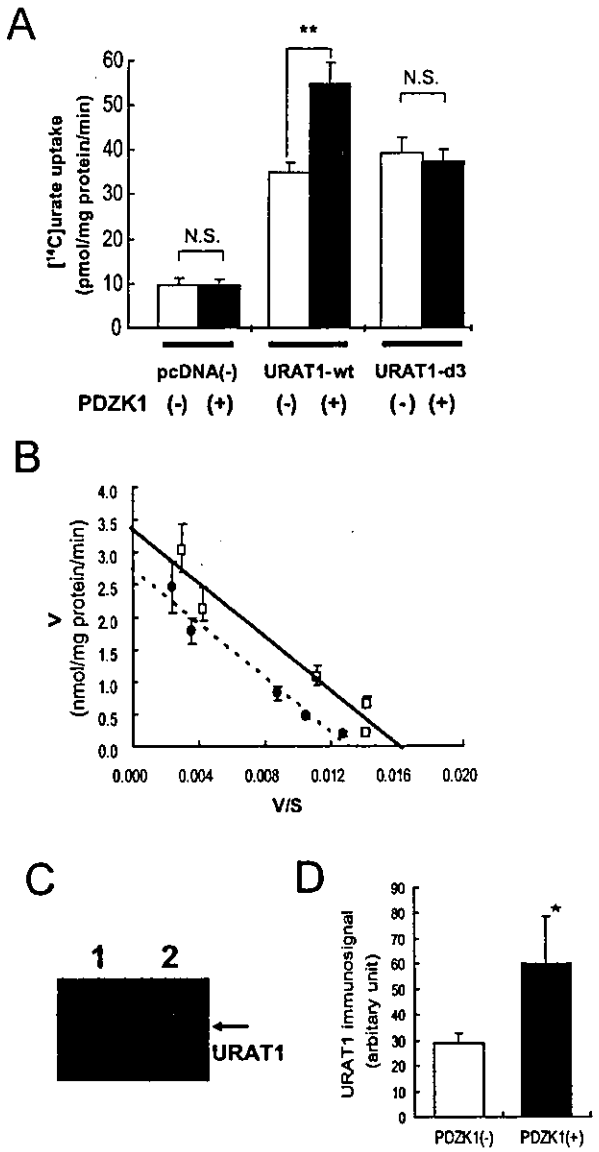

FIG. 6. **Effect of PDZK1 on [^{14}C]urate transport activity.** *A*, coexpression of URAT1 and PDZK1 increased urate uptake (20 μM) significantly in cells transfected with URAT1 alone. This effect was abolished when the C-terminal deletion mutant of URAT1 was cotransfected with PDZK1, confirming that the interaction of PDZK1 and the URAT1 C-terminal domain is responsible for this effect. **, $p < 0.01$; *d3*, mutant lacking the last three amino acids; *wt*, wild type; *N.S.*, not significant. *B*, kinetic data showed that PDZK1 (*open squares*) increased the V_{max} from 2.78 ± 0. 34 to 3.34 ± 0.25 nmol/mg protein/min ($p < 0.05$) and did not change the K_m (203.8 ± 25.6 to 198.7 ± 33.3 μM, $p = 0.78$) (*closed circles*). *V*, velocity; *V/S*, velocity per concentration of substrate. Each value represents the mean ± S.D. of four determinations from one typical experiment of the three separate experiments. *C*, cell surface biotinylation analysis of URAT1 stably expressing HEK293 cells transfected with vector alone (*lane 1*), and cells transfected with PDZK1 (*lane 2*). Single bands of ~45 kDa, which are consistent with URAT1, were observed in both lanes. *D*, quantification of immunosignal for URAT1 ($n = 3$, *error bars* are S.D.). *, $p < 0.05$.

have similar C-terminal amino acid sequences. SR-BI and MRP2 bind only to PDZ1 (27, 28), CFTR binds to PDZ1, PDZ3, and PDZ4 (14), and type IIa Na/P_i binds only to PDZ3 (26), whereas URAT1 binds to PDZ1, PDZ2, and PDZ4 (Figs. 1 and 2). Therefore, the observed interaction profile of the URAT1 C-terminal against each PDZ domain is unique and specific among PDZK1 partners.

The urate transport study revealed that the coexpression of PDZK1 with URAT1 in HEK293 cells leads to a significant enhancement of URAT1-mediated [^{14}C]urate transport. It was previously shown that PDZK1 potentiates CFTR chloride channel activity (13, 14). Recently, IKEPP, a PDZ domain protein closely related to PDZK1, was reported to alter the function of intestinal receptor guanylyl cyclase C (29). Therefore, the association of PDZK1 with URAT1 is an additional new example of the role of a PDZ-containing protein in modulating the function of their associated proteins (6–8). But the mechanism regarding PDZK1 modulation in URAT1 transport activity seems to be different from those two cases. Kinetic studies of urate transport showed a significant increase (1.4-fold) in V_{max} between PDZK1- and mock-transfected HEK293 cells (Fig. 6*B*). Therefore, PDZK1 may enhance urate transport either through an increase in the catalytic rate of the transporter or through an increase in cell surface availability. Cell surface biotinylation experiment revealed that the augmentation of the transport activity was associated with the increased surface expression level of URAT1 protein from HEK293 cells stably expressing URAT1 transfected with PDZK1 (Fig. 6*C*). These results suggested that PDZK1 stabilize and/or anchor URAT1 at the cell membrane, making it less likely to be internalized and subsequently degraded. However, we could not rule out the possibility derived from the studies of CFTR channel interactions with multi-PDZ domain protein CAP70 (mouse homologue of PDZK1) and NHERF (30). In two previous studies, it was concluded that PDZ domains in NHERF and CAP70 play a modulatory function by directly affecting CFTR channel gating: by linking the C termini of CFTR monomers within an NHERF PDZ1–2 or CAP70 PDZ3–4 tandem construct (dimerization) causes a further increase in open channel probability (13, 14). In the case of NHERF, no observable change in single-channel conductance or the number of channels is reported (13). As shown in Fig. 1*C*, because URAT1 can bind to PDZ1, PDZ2, and PDZ4 domains of PDZK1, it seems possible that the tandem PDZK1 PDZ1–2 domains form the dimer of URAT1 and the complex formation between URAT1 and the two PDZ domains of PDZK1 exerts its effect via allosteric modulation, as observed in the interaction of CFTR with both NHERF and PDZK1.

Kocher *et al.* (31) have recently reported the targeted disruption of the *PDZK1* gene. PDZK1-deficient mice displayed no gross phenotypic abnormalities, and no significant redistribution of proteins known to interact with PDZK1, such as MAP17, MRP2, and the type IIa Na/P_i cotransporter, was observed. They concluded that the absence of a more significant phenotype may be due to functional compensation by other PDZ-domain proteins. However, they did not perform the reverse transcription-PCR experiment against renal-specific transporter, mouse homologue of URAT1 (32, 33), and did not check the urate levels in both blood and urine. Further studies are required to evaluate the importance of PDZK1 for the urate transport system.

Very recently, Gisler *et al.* (34) performed the yeast two-hybrid screens using single PDZ domains derived from mouse PDZK1 (NaPi-Cap1) as bait and reported that, besides NaPi-IIa, mouse PDZK1 interacts with many other membrane transporters including RST (mouse URAT1) in the brush border of proximal tubular cells. Although they did not show the functional consequence of its interaction, these studies, combined with our results, indicate the physiological significance of the interaction between PDZK1 and URAT1 in the kidney.

In summary, we have identified that the PDZ domain protein PDZK1 is a binding partner of URAT1, which augments URAT1-mediated urate transport activity. A further study of transporter-interacting proteins, such as PDZ domain proteins, will better our understanding of the different regulation mechanisms of other transporters.

Acknowledgments—We thank Akie Toki for technical assistance. The anti-PDZK1 and anti-URAT1 polyclonal antibodies were supplied by Transgenic Inc., Kumamoto, Japan.

REFERENCES

1. Roch-Ramel, F., and Guisan, B. (1999) *News Physiol. Sci.* **14**, 80–84
2. Sica, D. A., and Schoolwerth, A. C. (2000) in *The Kidney* (Brenner, B. M., ed) 6th Ed., pp. 680–700, Saunders, Philadelphia
3. Maesaka, J. K., and Fishbane, S. (1998) *Am. J. Kidney Dis.* **32**, 917–933
4. Enomoto, A., Kimura, H., Chairoungdua, A., Shigeta, Y., Jutabha, P., Cha, S. H., Hosoyamada, M., Takeda, M., Sekine, T., Igarashi, T., Matsuo, H., Kikuchi, Y., Oda, T., Ichida, K., Hosoya, T., Shimotaka, K., Niwa, T., Kanai, Y., and Endou, H. (2002) *Nature* **417**, 447–452
5. Ichida, K., Hosoyamada, M., Hisatome, I., Enomoto, A., Hikita, M., Endou, H., and Hosoya, T. (2004) *J. Am. Soc. Nephrol.* **15**, 164–173
6. Hung, A. Y., and Sheng, M. (2002) *J. Biol. Chem.* **277**, 5699–5702
7. Garner, C. C., Nash, J., and Huganir, R. L. (2000) *Trends Cell Biol.* **10**, 274–280
8. Fanning, A. S., and Anderson, J. M. (1999) *Curr. Opin. Cell Biol.* **11**, 432–439
9. Harris, B. Z., and Lim, W. A. (2001) *J. Cell Sci.* **114**, 3219–3231
10. Songyang, Z., Fanning, A. S., Fu, C., Xu, J., Marfatia, S. M., Chishti, A. H., Crompton, A., Chan, A. C., Anderson, J. M., and Cantley, L. C. (1997) *Science* **275**, 73–77
11. Anzai, N., Deval, E., Schaefer, L., Friend, V., Lazdunski, M., and Lingueglia, E. (2002) *J. Biol. Chem.* **277**, 16655–16661
12. Jackson, M., Song, W., Liu, M.-Y., Jin, L., Dykes-Hoberg, M., Lin, C.-l. G., Bowers, W. J., Federoff, H. J., Sternweis, P. C., and Rothstein, J. D. (2001) *Nature* **410**, 89–93
13. Raghuram, V., Mak, D. D., and Foskett, J. K. (2001) *Proc. Natl. Acad. Sci. U. S. A.* **98**, 1300–1305
14. Wang, S., Yue, H., Derin, R. B., Guggino, W. B., and Li, M. (2000) *Cell* **103**, 169–179
15. Horio, Y., Hibino, H., Inanobe, A., Yamada, M., Ishii, M., Tada, Y., Satoh, E., Hata, Y., Takai, Y., and Kurachi, Y. (1997) *J. Biol. Chem.* **272**, 12885–12888
16. Kurschner, C., Mermelstein, P. G., Holden, W. T., and Surmeier, D. J. (1998) *Mol. Cell Neurosci.* **11**, 161–172
17. Malmqvist, M. (1993) *Nature* **361**, 186–187
18. Huh, K.-H., and Wenthold, R. J. (1999) *J. Biol. Chem.* **274**, 151–157
19. Kocher, O., Comella, N., Tognazzi, K., and Brown, L. F. (1998) *Lab. Invest.* **78**, 117–125
20. Weinman, E. J., Steplock, D., Wang, Y., and Shenolikar, S. (1995) *J. Clin. Invest.* **95**, 2143–2149
21. Reczek, D., Berryman, M., and Bretscher, J. (1997) *J. Cell Biol.* **139**, 169–179
22. Hall, R. A., Ostedgaard, L. S., Premont, R. T., Blitzer, J. T, Rahman, E., Welsh, M. J., and Lefkowitz, R. J. (1998) *Proc. Natl. Acad. Sci. U. S. A.* **95**, 8496–8501
23. Hosoyamada, M., Sekine, T., Kanai, Y., and Endou, H. (1999) *Am. J. Physiol.* **276**, F122–F128
24. Cha, S. H., Sekine, T., Kusuhara, H., Yu, E., Kim, J. Y., Kim, D. K., Sugiyama, Y., Kanai, Y., and Endou, H. (2000) *J. Biol. Chem.* **275**, 4507–4512
25. Cha, S. H., Sekine, T., Fukushima, J.-I., Kanai, Y., Kobayashi, Y., Goya, T., and Endou, H. (2001) *Mol. Pharmacol.* **59**, 1277–1286
26. Gisler, S. M., Stagljar, I., Traebert, M., Bacic, D., Biber, J., and Murer, H. (2001) *J. Biol. Chem.* **276**, 9206–9213
27. Ikemoto, M., Arai, H., Feng, D., Tanaka, K., Aoki, J., Dohmae, N., Takio, K., Adachi, H., Tsujimoto, M., and Inoue, K. (2000) *Proc. Natl. Acad. Sci. U. S. A.* **97**, 6538–6543
28. Kocher, O., Comella, N., Gilchrist, A., Pal, R., Tognazzi, K., Brown, L. F., and Knoll, J. H. M. (1999) *Lab. Invest.* **79**, 1161–1170
29. Scott, R. O., Thelin, W. R., and Milgram, S. L. (2002) *J. Biol. Chem.* **277**, 22934–22941
30. Bezprozvanny, I., and Maximov, A. (2001) *Proc. Natl. Acad. Sci. U. S. A.* **98**, 787–789
31. Kocher, O., Pal, R., Roberts, M., Cirovic, C., and Gilchrist, A. (2003) *Mol. Cell. Biol.* **23**, 1175–1180
32. Mori, K., Ogawa, Y., Ebihara, K., Aoki, T., Tamura, N., Sugawara, A., Kuwahara, T., Ozaki, S., Mukoyama, M., Tashiro, K., Tanaka, I., and Nakao, K. (1997) *FEBS Lett.* **417**, 371–374
33. Hosoyamada, M., Ichida, K., Enomoto, A., Hosoya, T., and Endou, H. (2004) *J. Am. Soc. Nephrol.* **15**, 261–268
34. Gisler, S. M., Pribanic, S., Bacic, D., Forrer, P., Gantenbein, A., Sabourin, L. A., Tsuji, A., Zhao, Z.-S., Manser, E., Biber, J., and Murer, H. (2003) *Kidney Int.* **64**, 1733–1745

Available online at www.sciencedirect.com
SCIENCE DIRECT
Neuroscience Research 50 (2004) 437–446
Neuroscience Research
www.elsevier.com/locate/neures

System L-amino acid transporters are differently expressed in rat astrocyte and C6 glioma cells

Do Kyung Kim[a,*], In Jin Kim[a], Shinae Hwang[b], Ji Hyun Kook[b], Min-Cheol Lee[b], Boo Ahn Shin[b], Choon Sang Bae[b], Jung Hoon Yoon[a], Sang Gun Ahn[a], Soo A Kim[a], Yoshikatsu Kanai[c], Hitoshi Endou[c], Jong-Keun Kim[b]

[a]*Department of Oral Physiology, Chosun University College of Dentistry, 375 Seosuk-dong, Dong-gu, Gwangju, 501-759, South Korea*
[b]*Chonnam National University Research Institute of Medical Sciences, Chonnam National University Medical School, Gwangju 501-746, South Korea*
[c]*Department of Pharmacology and Toxicology, Kyorin University School of Medicine, Tokyo 181-8611, Japan*

Received 21 June 2004; accepted 11 August 2004
Available online 17 September 2004

Abstract

The system L-amino acid transporter is a major nutrient transport system that is responsible for Na^+-independent transport of neutral amino acids including several essential amino acids. We have compared and examined the expressions and functions of the system L-amino acid transporters in both rat astrocyte cultures and C6 glioma cells. The rat astrocyte cultures expressed the L-type amino acid transporter 2 (LAT2) with its subunit 4F2hc, whereas the L-type amino acid transporter 1 (LAT1) was not expressed in these cells. The C6 glioma cells expressed LAT1 but not LAT2 with 4F2hc. The [^{14}C]L-leucine uptakes by the rat astrocyte cultures and C6 glioma cells were Na^+-independent and were completely inhibited by the system L selective inhibitor, BCH. These results suggest that the transport of neutral amino acids including several essential amino acids into rat astrocyte cultures and C6 glioma cells are for the most part mediated by LAT2 and LAT1, respectively. Therefore, the rat astrocyte cultures and C6 glioma cells are excellent tools for examining the properties of LAT2 and LAT1, respectively. Moreover, the specific inhibition of LAT1 in cancer cells might be a new rationale for anti-cancer therapy.

Keywords: L-Type amino acid transporter; Astrocyte cultures; C6 glioma cells; BCH; Essential amino acids; Anti-cancer therapy

1. Introduction

Amino acids are indispensable for the protein synthesis, which are essential for cell growth and proliferation in both normal and transformed cells (Christensen, 1990; McGivan and Pastor-Anglada, 1994). Amino acid transport across the plasma membrane is mediated via amino acid transporters located on the plasma membrane. Among the amino acid transport systems, the system L-amino acid transporter, which is a Na^+-independent neutral amino acid transport system, is a major route for providing living cells including tumor cells with neutral amino acids including several essential amino acids (Oxender and Christensen, 1963; Christensen, 1990). Because of its broad substrate selectivity, system L-amino acid transporter is regarded as a drug transporter that transports not only naturally occurring amino acids but also amino acid-related drugs such as L-dopa, a therapeutic drug for Parkinsonism; melphalan, an anti-cancer phenylalanine mustard; triiodothyronine and thyroxine, two thyroid hormones; gabapentin, an anticonvulsant; and *S*-(1,2-dichlorovinyl)-L-cysteine, a neurotoxic cysteine conjugate (Goldenberg et al., 1979; Christensen, 1990; Lakshmanan et al., 1990; Blondeau et al., 1993; Su et al., 1995; Gomes and Soares-da-Silva, 1999; Kanai and Endou, 2001).

Recently, the L-type amino acid transporter 1 and 2 (LAT1 and LAT2) were isolated (Kanai et al., 1998; Segawa et al., 1999; Yanagida et al., 2001). They were predicted to

Abbreviations: LAT1, L-type amino acid transporter 1; LAT2, L-type amino acid transporter 2; 4F2hc, 4F2 heavy chain; BCH, 2-aminobicyclo-(2,2,1)-heptane-2-carboxylic acid

* Corresponding author. Tel.: +82 62 230 6893; fax: +82 62 223 3205.
E-mail address: kdk@chosun.ac.kr (D.K. Kim).

0168-0102/$ – see front matter © 2004 Published by Elsevier Ireland Ltd and the Japan Neuroscience Society.
doi:10.1016/j.neures.2004.08.003

be 12-membrane-spanning proteins that mediate the exchange of Na^+-independent amino acids (Kanai et al., 1998; Segawa et al., 1999; Yanagida et al., 2001). LAT1 and LAT2 require an additional single-membrane-spanning protein, which is a heavy chain of the 4F2 antigen (4F2hc), for their functional expression in the plasma membrane (Kanai et al., 1998; Mannion et al., 1998; Mastroberardino et al., 1998; Pfeiffer et al., 1998; Nakamura et al., 1999; Segawa et al., 1999; Yanagida et al., 2001). LAT1 and 4F2hc or LAT2 and 4F2hc form a heterodimeric complex via a disulfide bond (Kanai et al., 1998; Mannion et al., 1998; Mastroberardino et al., 1998; Pfeiffer et al., 1998; Nakamura et al., 1999; Segawa et al., 1999; Yanagida et al., 2001). LAT1 mRNA is only expressed in restricted organs such as the brain, spleen, placenta and testis (Kanai et al., 1998; Nakamura et al., 1999; Prasad et al., 1999; Yanagida et al., 2001). In contrast, the mRNAs of LAT2 and 4F2hc are ubiquitously expressed in all normal embryonic and normal adult tissues (Kanai et al., 1998; Nakamura et al., 1999; Pineda et al., 1999; Rossier et al., 1999; Segawa et al., 1999; Yanagida et al., 2001). In addition, LAT1 is strongly expressed in malignant tumors presumably to support their continuous growth and proliferation (Sang et al., 1995; Wolf et al., 1996; Kanai et al., 1998; Yanagida et al., 2001). LAT1 prefers large neutral amino acids as its substrates (Kanai et al., 1998; Yanagida et al., 2001; Uchino et al., 2002). In contrast, LAT2 transports not only large neutral amino acids, but also small neutral amino acids, in a manner that appears to have broader substrate selectivity than LAT1 (Pineda et al., 1999; Rossier et al., 1999; Segawa et al., 1999; Rajan et al., 2000).

Based on what is mentioned above, it is proposed that the manipulation of the system L activity, in particular that of LAT1, might have anti-cancer therapeutic implications. The inhibition of LAT1 activity in tumor cells might be effective in the suppression of tumor cell growth by depriving of essential amino acids in tumor cells (Kanai and Endou, 2001; Kim et al., 2002a). Although the LAT1 activity in tumor cells is completely blocked, the growth and proliferation of normal cells is possible because the LAT2 is present in the normal cells.

The availability of in vitro assay systems for examining the interaction with LAT1 and LAT2 will facilitate the development of such drugs. The functional properties of LAT1 and LAT2 have been studied formerly by injecting their cRNAs into *Xenopus* oocytes or by transiently transfecting their cDNAs into cultured mammalian cells, which is not well-suited for the efficient screening of chemical compounds (Kanai et al., 1998; Mastroberardino et al., 1998; Nakamura et al., 1999; Prasad et al., 1999; Segawa et al., 1999; Yanagida et al., 2001; Uchino et al., 2002). Furthermore, there are few studies that compared the expression and functional characterization of amino acid transporters including the system L-amino acid transporters for supplying nutrients to normal cells and cancer cells.

In the present study, therefore, we examined and compared the expressions of system L-amino acid transporters as well as the properties of the L-leucine transport in the rat astrocyte cultures and C6 glioma cells. The results showed that the transport of neutral amino acids including several essential amino acids into the rat astrocyte cultures and C6 glioma cells were almost exclusively mediated by LAT2 and LAT1, respectively, Therefore, the rat astrocyte cultures and C6 glioma cells might be the excellent tools for both examining and comparing the interaction of chemical compounds with LAT2 and LAT1. The specific inhibition of LAT1 might also be a new rationale for examining new anti-cancer therapies.

2. Materials and methods

2.1. Materials

The [^{14}C]L-leucine was purchased from Perkin-Elmer Life Sciences Inc. (Boston, MA, USA). The affinity-purified rabbit anti-rat LAT1, anti-rat LAT2 and anti-rat 4F2hc polyclonal antibodies were kindly provided by Kumamoto Immunochemical Laboratory, Transgenic Inc. (Kumamoto, Japan). The 2-aminobicyclo-(2,2,1)-heptane-2-carboxylic acid (BCH) and other chemicals were purchased from Sigma (St. Louis, MO, USA).

2.2. Cell lines and cell cultures

The rat C6 glioma cells were provided by American Type Culture Collection (ATCC, Rockville, MD, USA) and were grown in DMEM supplemented with 10% FBS and the appropriate concentrations of antibiotics (100 U/ml penicillin and 100 μg/ml streptomycin) (Gravel et al., 2000; Yan et al., 2001). The cells were maintained as monolayers in plastic culture plate at 37 °C in a humidified atmosphere containing 5% CO_2.

The primary astrocyte cultures were prepared from neonatal rats (Wistar, Daehan Biolink, Choongbuk, Korea) according to the method described elsewhere (Abe and Saito, 2000) with minor modifications. Cerebral hemispheres of postnatal day 1–2 pups were freed from the meninges, the hippocampus and the choroids plexus. The cortices were dissociated with trypsin digestion. For uptake experiments, the cortical cells were plated in 24-well plate at a density of 2.5×10^4 cells per well in minimal essential medium (MEM; Earles salts, supplied bicarbonate- and glutamine-free) supplemented with 21 mM glucose, 2 mM glutamine, 26.5 mM bicarbonate, 10% fetal bovine serum, 10% horse serum and 10 ng/ml epidermal growth factor. For RT-PCR or Western blot analysis, the cells were plated in plastic dishes of 100 mm diameter at the density of 1×10^6 cells per dish. The cultures were then maintained 2–3 weeks in a humidified incubator with 5% CO_2 at 37 °C until the cultures were mature and confluent. All efforts were made to minimize animal suffering as well as the number of animal used (Wilhelm et al., 2004).

2.3. RT-PCR analysis

The RNAs were prepared from the rat astrocyte cultures and C6 glioma cells maintained in the growth medium at 37 °C using RNA preparation kits (Isogen, Nippon-Gene, Japan), in accordance with the manufacturer's instruction. The poly(A)$^+$RNAs were selected by oligo(dT) cellulose chromatography (Utsunomiya-Tate et al., 1996).

For RT-PCR analysis, the first-strand cDNAs were prepared from the rat astrocyte cultures and C6 glioma cell poly(-A)$^+$RNAs using the SuperScript First-Strand Synthesis System for RT-PCR (Life Technologies Inc., CA, USA) with an oligo(dT) primer, and were used as a template for PCR amplification. The PCR amplification was performed using Taq polymerase Amplitaq Gold (Roche Molecular Systems Inc., Germany) according to the following protocol: 94 °C for 12 min, followed by 25 cycles of 94 °C for 30 s, 60 °C for 30 s and 72 °C for 40 s and a final extension step of 72 °C for 30 min (Birch, 1996; Kim et al., 2002b). A pair of primers, 5′-CAATGGTGTGGCCATCATAG-3′ (162–181 bp of coding region) and 5′-GATGCATCCCCTTGTCCTAT-3′ (670–689 bp of coding region), were used for PCR the amplification of rat LAT1. A pair of primers, 5′-TCATTGGCTCCGGAATCTTC-3′ (161–180 bp of coding region) and 5′-ATGCATTCTTTGGCTCCAGC-3′ (651–670 bp of coding region), were used for the PCR amplification of rat LAT2. A pair of primers, 5′-TCACAGGCTTATCCAAGGAG-3′ (161–180 bp of coding region) and 5′-TACAATGTCAGCCTGAGGAG-3′ (641–660 bp of coding region), were used for the PCR amplification of rat 4F2hc.

2.4. Western blot analysis

The protein samples from the rat astrocyte cultures and C6 glioma cells were prepared as described elsewhere (Chairoungdua et al., 1999; Kim et al., 2001; Yanagida et al., 2001) with minor modifications. The protein samples were heated at 100 °C for 5 min in a sample buffer, either in the presence (reducing condition) or absence (nonreducing condition) of 5% 2-mercaptoethanol, and then subjected to SDS–polyacrylamide gel electrophoresis. The separated proteins were transferred electrophoretically to a Hybond-P polyvinylidene difluoride transfer membrane. The membrane was treated with nonfat dried milk and diluted anti-rat LAT1 (1:250 dilution), anti-rat LAT2 (1:250 dilution) and anti-rat 4F2hc (1:500 dilution) affinity-purified antibodies (Matsuo et al., 2000; Tamai et al., 2001), and then with horseradish peroxidase-conjugated anti-rabbit IgG as a secondary antibody. The signals were detected using an ECL plus system (Amersham Pharmacia Biotech, NJ, USA) (Chairoungdua et al., 1999; Kim et al., 2001; Kim et al., 2002a; Yoon et al., 2004).

2.5. Uptake measurements in rat astrocyte cultures C6 glioma cells

To characterize the function of the endogenously expressed system L amino acid transporters in the rat astrocyte cultures and C6 glioma cells, uptake experiments were performed as described elsewhere (Kim et al., 2002a; Yoon et al., 2004). The rat astrocyte cultures and C6 glioma cells were maintained in a growth medium at 37 °C in 5% CO_2. The C6 glioma cells were collected and seeded on 24-well plates (1×10^5 cells/well) in fresh growth medium. The uptake measurements were performed when the cells reached approximately 85–95% confluence on 24-well plates. The rat astrocyte cultures were used for the uptake experiments at 13–15 days in vitro.

After removing the growth medium, the cells were washed three times with a standard uptake solution (125 mM NaCl, 4.8 mM KCl, 1.3 mM $CaCl_2$, 1.2 mM $MgSO_4$, 25 mM HEPES, 1.2 mM KH_2PO_4 and 5.6 mM glucose, pH 7.4) or Na^+-free uptake solution (125 mM choline–Cl, 4.8 mM KCl, 1.3 mM $CaCl_2$, 1.2 mM $MgSO_4$, 25 mM HEPES, 1.2 mM KH_2PO_4 and 5.6 mM glucose, pH 7.4), and preincubated for 10 min at 37 °C. The medium was then replaced by the uptake solution containing [^{14}C]L-leucine. The uptake was terminated by removing the uptake solution followed by washing the plates three times with the ice-cold uptake solution. The cells were then solubilized with 0.1 N NaOH and the radioactivity was counted by liquid scintillation spectrometry. The values are expressed as pmol/mg protein/min. Four to six-wells of cells were used for each data point in order to measure the uptake of [^{14}C]L-leucine. In order to confirm the reproducibility of the results, three or four separate experiments were performed for each measurement. The results shown in the figures are from these representative experiments.

The K_m and V_{max} values were determined using Eadie–Hofstee plots based on the [^{14}C]L-leucine uptakes measured for 1 min at 10, 30, 100, 300, 1000 and 3000 μM for the rat astrocyte cultures and C6 glioma cells.

The IC_{50} values for BCH on the L-leucine transport were determined on the 1 μM [^{14}C]L-leucine uptake measured for 1 min in the presence of 0, 10, 30, 100, 300, 1000 and 3000 μM BCH.

To measure the K_i values for BCH, the uptake rates of [^{14}C]L-leucine were measured for 1 min at various concentrations of [^{14}C]L-leucine (10, 30, 100, 300, 1000 and 3000 μM) with or without the addition of 100 μM BCH. The K_i values were determined by double reciprocal plot analysis where 1/uptake rate of [^{14}C]L-leucine was plotted against the 1/L-leucine concentration. The K_i values were calculated from the following equation when a competitive inhibition was observed: K_i = concentration of inhibitor/((K_m of L-leucine with the inhibitor/K_m of L-leucine without the inhibitor)-1) (Kim et al., 2002a; Uchino et al., 2002).

For the inhibition experiments, the uptake of 30 μM [^{14}C]L-leucine uptake was measured in the presence or absence of the 3 mM non-labeled L-amino acids and BCH.

2.6. Data analysis

All the experiments were performed at least in triplicate. The results are presented as mean ± S.E.M.

3. Results

3.1. Detection of system L-amino acid transporters in rat astrocyte cultures and C6 glioma cells

In the RT-PCR analysis, the PCR products for LAT2 and their associating protein 4F2hc were detected in the rat astrocyte cultures (Fig. 1A). In the rat astrocyte cultures, the signal for the product of LAT1 was not detected (Fig. 1A). In the C6 glioma cells, the PCR products for the LAT1 and 4F2hc were detected, whereas that for the LAT2 was not (Fig. 1B).

Western blot analysis was performed on the membrane fractions prepared from the rat astrocyte cultures and C6 glioma cells. In the rat astrocyte cultures, the antibodies raised against LAT2 and 4F2hc recognized the approximately 125–135 kDa protein band under nonreducing conditions, whereas, under reducing conditions, these bands shifted to the 47 and 85 kDa protein bands for LAT2 and 4F2hc, respectively (Fig. 2A). The protein band for LAT1 was not detected in the membrane fractions prepared from the rat astrocyte cultures under both reducing and nonreducing conditions (Fig. 2A). In the C6 glioma cells, the antibodies raised against LAT1 and 4F2hc both recognized the 125–135 kDa protein band under nonreducing conditions, whereas this band shifted to the 40 and 85 kDa protein bands for LAT1 and 4F2hc, respectively, under reducing conditions (Fig. 2B). The protein band for LAT2 was not detected in the membrane fractions prepared from the C6 glioma cells under the reducing and nonreducing conditions (Fig. 2B).

The results from the RT-PCR and Western blot analyses indicate that LAT2, but not LAT1, is present together with 4F2hc in the rat astrocyte cultures and LAT1, but not LAT2, is present with 4F2hc in the C6 glioma cells.

3.2. The [^{14}C]L-leucine uptake by rat astrocyte cultures and C6 glioma cells

The [^{14}C]L-leucine transport was examined in the rat astrocyte cultures and C6 glioma cells. As shown in Fig. 3A, the level of [^{14}C]L-leucine (30 μM) uptake by the rat

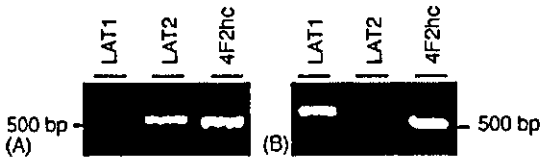

Fig. 1. Detection of LAT1, LAT2 and 4F2hc by RT-PCR in the rat astrocyte cultures and C6 glioma cells. The first strand cDNAs prepared from the rat astrocyte cultures (A) and C6 glioma cell (B) poly(A)$^+$RNAs were used as templates for PCR amplification. The PCR products were subjected to electrophoresis on a 1.2% agarose gel and visualized with ethidium bromide. The LAT2-specific PCR product (509 bp) and the 4F2hc-specific PCR product (499 bp) were obtained from the rat astrocyte cultures (A). The LAT1-specific PCR product (529 bp) and 4F2hc-specific PCR product (499 bp) were obtained from the C6 glioma cells (B).

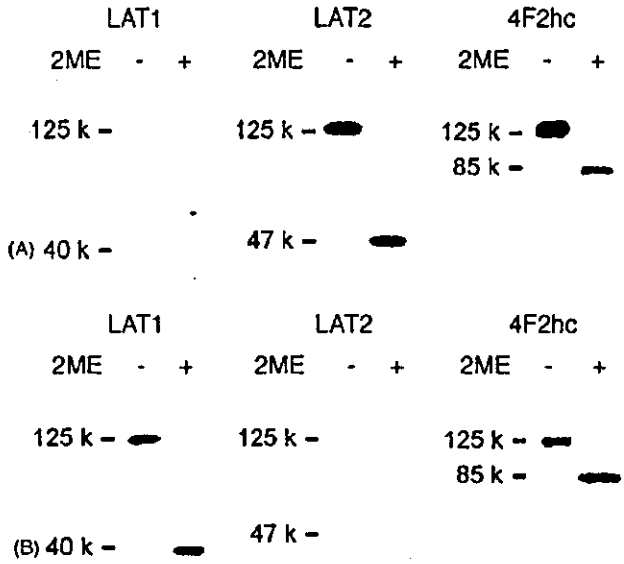

Fig. 2. Associations between the LAT2 and 4F2hc proteins in the rat astrocyte cultures and the LAT1 and 4F2hc proteins in the C6 glioma cells. Western blot analyses were performed on the membrane fractions prepared from the rat astrocyte cultures (A) and C6 glioma cells (B) in the presence or absence of 2-mercaptoethanol, using anti-LAT1, anti-LAT2 and anti-4F2hc antibodies. In the rat astrocyte cultures (A), for LAT2, the 125–135 kDa protein band detected in the absence of 2-mercaptoethanol ('2ME-') shifted to a 47 kDa protein band by treatment with 2-mercaptoethanol ('2ME+'). For 4F2hc, the 125–135 kDa protein band detected in the absence of 2-mercaptoethanol ('2ME-') shifted to an 85 kDa protein band by treatment with 2-mercaptoethanol ('2ME+'). For LAT1, no protein band was detected in both the presence ('2ME+') and absence ('2ME-') of 2-mercaptoethanol. In the C6 glioma cells (B), for LAT1, the 125 kDa protein band detected in the absence of 2-mercaptoethanol ('2ME-') was not detected in the presence of 2-mercaptoethanol ('2ME+'), but a 40 kDa protein band was detected instead. For 4F2hc, the 125 kDa protein band detected in the absence of 2-mercaptoethanol ('2ME-') shifted to an 85 kDa protein band by treatment with 2-mercaptoethanol ('2ME+'). For LAT2, no protein band was detected in both the presence ('2ME+') and absence ('2ME-') of 2-mercaptoethanol.

astrocyte cultures and C6 glioma cells measured in the standard uptake solution (Na) was not altered by replacing NaCl in the uptake solution with choline–Cl (Choline), indicating that the L-leucine uptake by the rat astrocyte cultures and C6 glioma cells is mostly Na^+-independent. In the subsequent experiments, the transport measurements were performed under Na^+-free conditions. The [^{14}C]L-leucine (30 μM) uptake was not detected when the uptake measurements were performed on ice, confirming that the [^{14}C]L-leucine uptake by rat astrocyte cultures and C6 glioma cells was due to the transporter-mediated transport (Fig. 3A). In the Na^+-free condition, the level of [^{14}C]L-leucine (30 μM) uptake was higher in the C6 glioma cells (2615 ± 100 pmol/mg protein/min) than in the rat astrocyte cultures (1996 ± 63 pmol/mg protein/min) (Fig. 3A). In the rat astrocyte cultures and C6 glioma cells, the uptake of [^{14}C]L-leucine (30 μM) was almost completely inhibited by 3 mM BCH, a specific inhibitor of the system L-amino acid transporters (Fig. 3B), indicating that the system L-amino

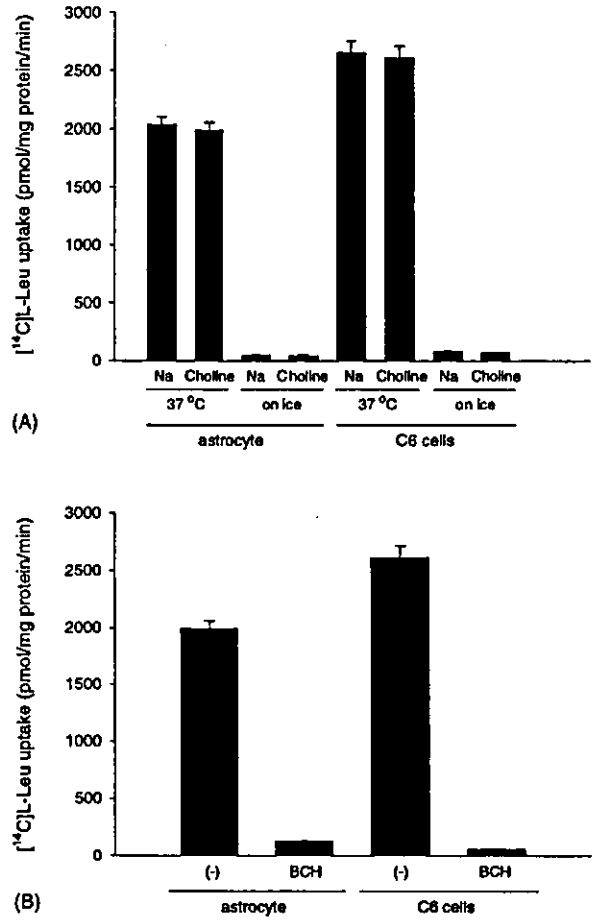

Fig. 3. The [^{14}C]L-leucine uptake and inhibition of [^{14}C]L-leucine transport by BCH in the rat astrocyte cultures and C6 glioma cells. (A) The ion dependence of [^{14}C]L-leucine transport. The [^{14}C]L-leucine (30 μM) uptake measured in the standard uptake solution (Na) was compared with the measured in the Na^+-free uptake solution (Choline) in the rat astrocyte cultures (astrocyte) and C6 glioma cells (C6 cells). The [^{14}C]L-leucine transport measurement was performed at either 37 °C or on ice. (B) The inhibition of [^{14}C]L-leucine transport by 2-aminobicyclo-(2,2,1)-heptane-2-carboxylic acid (BCH), a specific inhibitor of system L-amino acid transporters. The [^{14}C]L-leucine (30 μM) uptake was measured in the presence (BCH) or absence (–) of 3 mM BCH.

acid transporter is responsible for the [^{14}C]L-leucine uptake in the rat astrocyte cultures and C6 glioma cells.

In order to determine the time course of [^{14}C]L-leucine uptake by the rat astrocyte cultures and C6 glioma cells, the level of [^{14}C]L-leucine (30 μM) uptake was measured for 0.5, 1, 2.5, 5, 10 and 20 min (Fig. 4). The uptake of [^{14}C]L-leucine (30 μM) was time-dependent and exhibited a linear dependence on the incubation time up to 1 min in both the rat astrocyte cultures and C6 glioma cells (Fig. 4); all the subsequent uptake measurements were conducted for 1 min and the values are expressed as pmol/mg protein/min.

As shown in Fig. 5A, the [^{14}C]L-leucine uptake was saturable and followed Michaelis–Menten kinetics with a K_m value of 224.2 ± 39.8 μM (mean ± S.E.M. of three

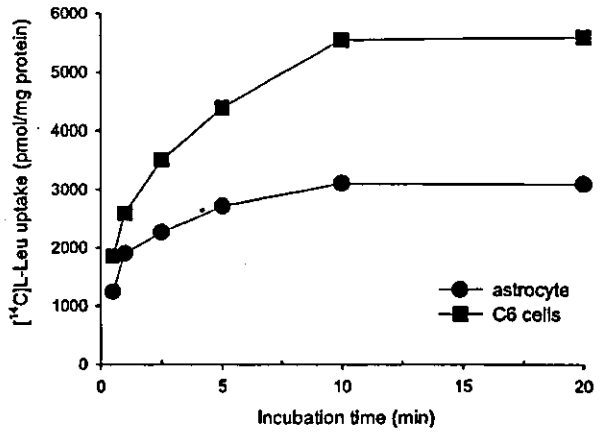

Fig. 4. Time course of [^{14}C]L-leucine uptake by rat astrocyte cultures and C6 glioma cells. The rat astrocyte cultures (astrocyte, filled circle) and C6 glioma (C6 cells, filled square) cells were incubated in the Na^+-free uptake solution containing 30 μM [^{14}C]L-leucine for 0.5, 1, 2.5, 5, 10 and 20 min.

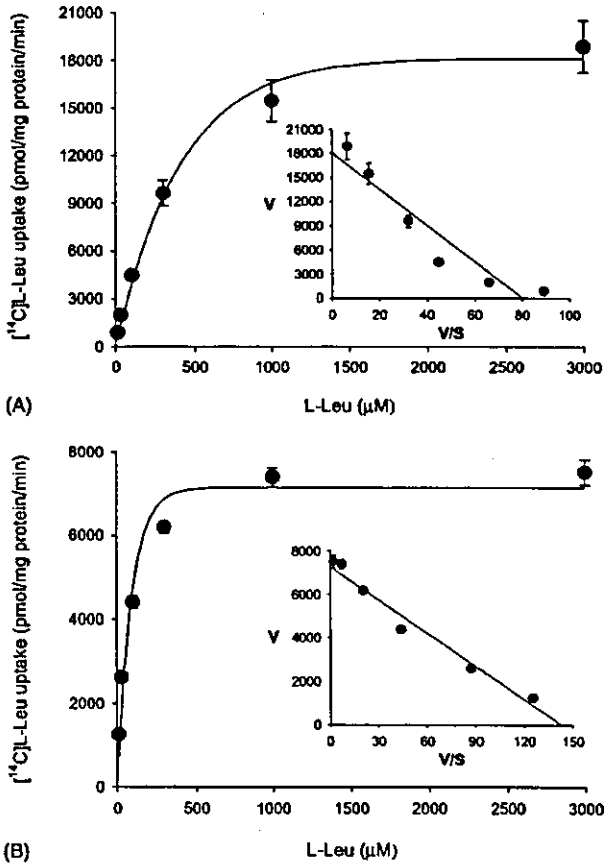

Fig. 5. The concentration dependence of [^{14}C]L-leucine transport in the rat astrocyte cultures and C6 glioma cells. The [^{14}C]L-leucine uptakes by the rat astrocyte cultures (A) and C6 glioma cells (B) were measured for 1 min and plotted against the L-leucine concentration. The L-leucine uptakes were saturable and fit the Michaelis–Menten curves in the rat astrocyte cultures (K_m = 224.2 μM; V_{max} = 18033.0 pmol/mg protein/min) (A) and C6 glioma cells (K_m = 52.1 μM; V_{max} = 7388.3 pmol/mg protein/min) (B). The insets show Eadie–Hofstee plots of the L-leucine uptake that were used to determine the kinetic parameters.

separate experiments) for the [^{14}C]L-leucine uptake in the rat astrocyte cultures. In the C6 glioma cells, the [^{14}C]L-leucine uptake was also saturable and followed Michaelis–Menten kinetics with a K_m value of 52.1 ± 6.9 μM (mean ± S.E.M. of three separate experiments) for the [^{14}C]L-leucine uptake (Fig. 5B).

3.3. Inhibition of [^{14}C]L-leucine uptake by BCH in rat astrocyte cultures and C6 glioma cells

In order to examine which BCH interacts with the L-leucine uptake mechanism in rat astrocyte cultures and C6 glioma cells, the [^{14}C]L-leucine (1 μM) uptake was measured in the presence of various BCH concentrations (0, 10, 30, 100, 300, 1000 and 3000 μM) and the [^{14}C]L-leucine uptake rate was measured at various [^{14}C]L-leucine concentrations (10, 30, 100, 300, 1000 and 3000 μM) with or without the addition of 100 μM BCH.

As shown in Fig. 6, the BCH (1–3000 μM) inhibited the [^{14}C]L-leucine (1 μM) uptake in a concentration-dependent manner with IC_{50} values of 270.2 ± 13.7 μM (rat astrocyte cultures, mean ± S.E.M. of three separate experiments) and 73.1 ± 4.5 μM (C6 glioma cells, mean ± S.E.M. of three separate experiments) in the rat astrocyte cultures and C6 glioma cells, respectively. In the rat astrocyte cultures and C6 glioma cells, the inhibition of [^{14}C]L-leucine uptake by BCH was shown to be competitive in a double reciprocal plot analysis with K_i values of 228.5 ± 39.7 μM (rat astrocyte cultures, mean ± S.E.M. of four separate experiments) (Fig. 7A) and 55.1 ± 7.9 μM (C6 glioma cells, mean ± S.E.M. of four separate experiments) (Fig. 7B), respectively.

The results from the uptake experiments indicate that the affinity for substrate uptake is higher in the C6 glioma cells expressing LAT1 as the system L-amino acid transporter than

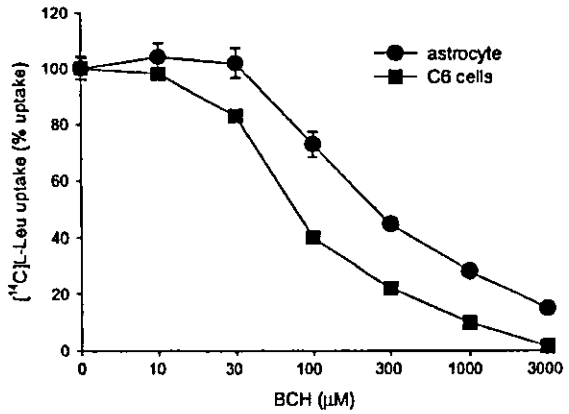

Fig. 6. Concentration-dependent inhibition of [^{14}C]L-leucine uptake by BCH in the rat astrocyte cultures and C6 glioma cells. The [^{14}C]L-leucine uptake (1 μM) was measured for 1 min in the presence of various BCH concentrations in the rat astrocyte cultures (astrocyte, filled circle) and C6 glioma cells (C6 cells, filled square), and is expressed as a percentage of the control-L-leucine uptake in the absence of BCH.

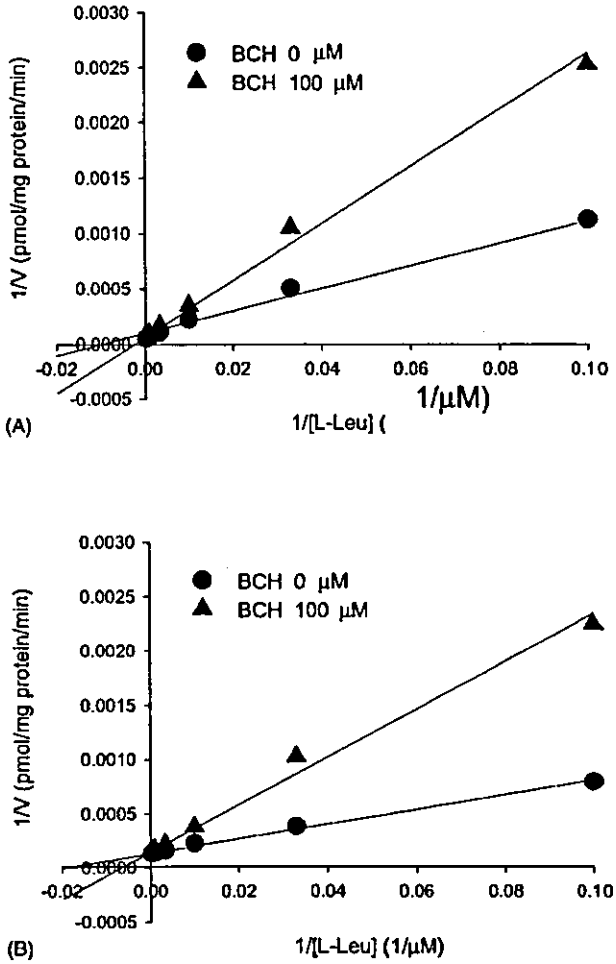

Fig. 7. Double reciprocal plot analyses of the inhibitory effect of BCH on the [^{14}C]L-leucine uptake in the rat astrocyte cultures and C6 glioma cells. The [^{14}C]L-leucine uptakes (10, 30, 100, 300, 1000 and 3000 μM) were measured in the presence (filled triangle) or absence (filled circle) of 100 μM BCH in the rat astrocyte cultures (A) and C6 glioma cells (B).

in the rat astrocyte cultures expressing LAT2 as the system L-amino acid transporter.

3.4. Inhibition of [^{14}C]L-leucine uptake by L-amino acids in rat astrocyte cultures and C6 glioma cells

In order to examine which L-amino acids interact with L-leucine uptake mechanism in the rat astrocyte cultures and C6 glioma cells, the [^{14}C]L-leucine (30 μM) uptake was measured in the presence of 3 mM non-labeled L-amino acids in the Na^+-free uptake solution.

The [^{14}C]L-leucine uptake was markedly inhibited by the L-isomers of alanine, serine, threonine, cysteine, asparagine, glutamine methionine, leucine, isoleucine, valine, phenylalanine, tyrosine, tryptophan and histidine in the rat astrocyte cultures cells (Fig. 8A), which is, in principle, consistent

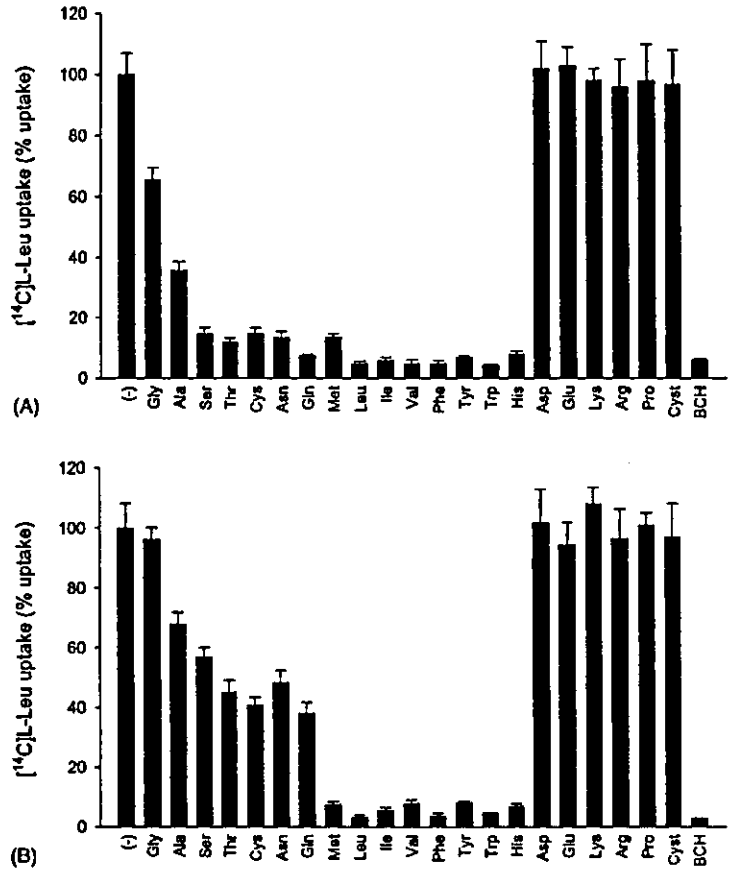

Fig. 8. Inhibition of [^{14}C]L-leucine uptake by the L-amino acids in the rat astrocyte cultures and C6 glioma cells. The [^{14}C]L-leucine (30 μM) uptake was measured in the presence of 3 mM non-radiolabeled L-amino acids and the system L specific inhibitor, BCH, in the rat astrocyte cultures (A) and C6 glioma cells (B).

with the properties of LAT2 expressed in the *Xenopus* oocytes (Pineda et al., 1999; Segawa et al., 1999).

The [^{14}C]L-leucine uptake was strongly inhibited by the L-isomers of methionine, leucine, isoleucine, valine, phenylalanine, tyrosine, tryptophan and histidine in the C6 glioma cells (Fig. 8B). In the C6 glioma cells, threonine, cysteine, asparagine and glutamine and some other L-amino acids exhibited weaker inhibitory effects on [^{14}C]L-leucine transport (Fig. 8B), which is, in principle, consistence with the properties of LAT1 expressed in the *Xenopus* oocytes (Kanai et al., 1998; Yanagida et al., 2001; Uchino et al., 2002).

4. Discussion

In the present study, we investigated and compared the expressions of the system L-amino acid transporters and the properties of L-leucine transport on the rat astrocyte cultures and C6 glioma cells.

By RT-PCR analysis, we demonstrated that the rat astrocyte cultures express LAT2, which is an isoform of the system L-amino acid transporter, at high levels together with its associated protein, 4F2hc, but do not express the other system L isoform, LAT1 (Fig. 1). The C6 glioma cells were shown to express LAT1 together with its associated protein, 4F2hc, but not LAT2 (Fig. 1). The proteins for LAT2 and 4F2hc were connected to each other via a disulfide bond on the membrane fraction prepared from the rat astrocyte cultures, which were detected by western blot analyses (Fig. 2). In contrast to the rat astrocyte cultures, the C6 glioma cells expressed the LAT1 protein together with its associating protein, 4F2hc, which were also connected to each other via a disulfide bond (Fig. 2). In our previous study, we reported that T24 human bladder carcinoma cells and KB human oral epidermoid carcinoma cells express LAT1 and 4F2hc, but not LAT2 (Kim et al., 2002a; Yoon et al., 2004). In addition, the LAT1 is highly expressed in malignant tumors presumably to support their continuous growth and proliferation (Sang et al., 1995; Wolf et al., 1996; Kanai et al., 1998; Yanagida et al., 2001). Although the LAT1 is expressed in the brain, the LAT1 is expressed mainly in the blood–brain barrier (Boado et al., 1999; Matsuo et al., 2000). As the results in this study correspond

with those of our previous reports (Kim et al., 2002a; Yoon et al., 2004), it is concluded that the rat astrocyte cultures, as normal cells, express only LAT2 with 4F2hc. However, the C6 glioma cells, as cancer cells, express only LAT1 with 4F2hc.

The [^{14}C]L-leucine uptakes measured in the rat astrocyte cultures and C6 glioma cells were Na^+-independent and were almost completely inhibited by the selective inhibitor of the system L-amino acid transporters, BCH (Fig. 3). This suggests that system L-amino acid transporters mediate the majority of L-leucine transport in the rat astrocyte cultures and C6 glioma cells. The level of [^{14}C]L-leucine uptake was higher in the C6 glioma cells than in the rat astrocyte cultures (Fig. 4). The [^{14}C]L-leucine uptakes by the rat astrocyte cultures and C6 glioma cells were saturable and followed Michaelis-Menten kinetics (Fig. 5). The K_m values of the rat astrocyte cultures and C6 glioma cells for the [^{14}C]L-leucine uptake were approximately 224 μM and 52 μM, respectively. The K_m value (52 μM) of the C6 glioma cells was relatively higher than those for the human LAT1 (19.7 μM) (Yanagida et al., 2001) and rat LAT1 (18.1 μM) (Kanai et al., 1998; Uchino et al., 2002) expressed in the *Xenopus* oocytes, and this small difference may be due to the different cell systems and conditions used (Kanai et al., 1998; Yanagida et al., 2001; Uchino et al., 2002). The K_m value (224 μM) of the rat astrocyte cultures was similar to that of the human LAT2 (220 μM) (Pineda et al., 1999) expressed in the *Xenopus* oocytes, but was relatively higher than that of the rat LAT2 (120 μM) (Segawa et al., 1999) expressed in the *Xenopus* oocytes. This difference may also be due to the different cell systems and conditions used (Pineda et al., 1999; Segawa et al., 1999). Although the small differences exist, the K_m value for the rat astrocyte cultures was similar to those of human LAT2 (Pineda et al., 1999) and rat LAT2 (Segawa et al., 1999) expressed in the *Xenopus* oocytes, and the K_m value for the C6 glioma cells was similar to those of human LAT1 (Yanagida et al., 2001) and rat LAT1 (Kanai et al., 1998; Uchino et al., 2002) expressed in the *Xenopus* oocytes. In addition, the affinity for L-leucine transport was apparently higher in the C6 glioma cells than in the rat astrocyte cultures.

BCH is an amino acid-related compound that has been used as a selective inhibitor of the system L-amino acid transporters including LAT1 and LAT2 (Christensen et al., 1969; Christensen, 1990; Kim et al., 2002a). Although BCH is the selective inhibitor of system L, BCH also inhibits the transports of the amino acids mediated by a Na^+-dependent neutral and basic amino acid transporter, $ATB^{0,+}$ (Sloan and Mager, 1999). In the Na^+-free condition, however, it is still correct that BCH selectively inhibits the transports of amino acids mediated by the system L-amino acid transporters. In this study, BCH completely inhibited the [^{14}C]L-leucine uptake measured in the rat astrocyte cultures and C6 glioma cells (Fig. 3, Figs. 6 and 7). The [^{14}C]L-leucine uptakes by the rat astrocyte cultures and C6 glioma cells were inhibited by BCH in a concentration-dependent fashion (Fig. 6). The inhibitions were shown to be competitive with the K_i values of 228.5 μM and 55.1 μM in the rat astrocyte cultures and C6 glioma cells, respectively (Fig. 7). The affinity for BCH against L-leucine transport was higher in the C6 glioma cells than in the rat astrocyte cultures. The C6 glioma cells expressed only LAT1 as the system L-amino acid transporter, whereas the rat astrocyte cultures expressed only LAT2 as the system L-amino acid transporters. These results suggest that the LAT2 plays an important role in the L-leucine uptake in the rat astrocyte cultures, as normal cells, and the LAT1 plays an important role in the L-leucine uptake in the C6 glioma cells, as cancer cells.

The [^{14}C]L-leucine uptakes by the rat astrocyte cultures and C6 glioma cells were markedly inhibited by the L-isomers of almost all the neutral amino acids and the L-isomers of only the large neutral amino acids, respectively (Fig. 8). The profiles of the inhibition of [^{14}C]L-leucine uptake by the L-amino acids in the rat astrocyte cultures and C6 glioma cells were similar to those determined for the LAT2 of human (Pineda et al., 1999) and rat (Segawa et al., 1999) expressed in the *Xenopus* oocytes and for the LAT1 of human (Yanagida et al., 2001) and rat (Kanai et al., 1998; Uchino et al., 2002) expressed in the *Xenopus* oocytes, respectively. As already mentioned, LAT2 and LAT1 are the main system L-amino acid transporter in the rat astrocyte cultures and C6 glioma cells, respectively. Taken together, it is concluded that the majority of [^{14}C]L-leucine uptake is mediated by LAT2 and LAT1 with their associated protein, 4F2hc, in the rat astrocyte cultures and C6 glioma cells, respectively. These results also suggest that the rat astrocyte cultures and C6 glioma cell systems are excellent tools to investigate for transport properties of various compounds via LAT2 and LAT1, respectively.

In the present study, we have characterized and compared the expressions of the system L-amino acid transporters and the properties of the L-leucine transport in the rat astrocyte cultures and C6 glioma cells. Furthermore, we have demonstrated that the subtype of system L-amino acid transporters mainly expressed in the rat astrocyte cultures and C6 glioma cells is different. Also, it is suggested that the transport of neutral amino acids including several essential amino acids into the rat astrocyte cultures and C6 glioma cells is mediated mainly by LAT2 and LAT1, respectively. The LAT1 is upregulated in tumor cells to support their continuous growth and proliferation (Sang et al., 1995; Wolf et al., 1996; Kanai et al., 1998; Yanagida et al., 2001). Therefore, LAT1 is a major route through which the C6 glioma cells, as cancer cells, gather up large neutral amino acids including several essential amino acids to support their continuous growth and proliferation. Although the LAT1 activity in tumor cells is completely blocked, the growth and proliferation of normal cells is possible because the LAT2 is present in the normal cells. Therefore, the specific inhibition of LAT1 would be a new rationale for the suppression of tumor cell growth including that of C6 glioma cells.

Overall, the results of the present study demonstrate that the transport of neutral amino acids including several essential amino acids into the rat astrocyte cultures and C6 glioma cells are mediated mainly by LAT2 and LAT1, respectively, and the LAT1 would be a new target for the inhibition of glioma cell growth.

Acknowledgements

This work was supported by Korea Research Foundation Grant (KRF-2003-003-E00010). The anti-rat LAT1, anti-rat LAT2 and anti-rat 4F2hc polyclonal antibodies were supplied by Kumamoto Immunochemical Laboratory, Transgenic Inc., Kumamoto, Japan.

References

Abe, K., Saito, H., 2000. The p44/42 mitogen-activated protein kinase cascade is involved in the induction and maintenance of astrocyte stellation mediated by protein kinase C. Neurosci. Res. 36, 251–257.

Birch, D.E., 1996. Simplified hot start PCR. Nature 381, 445–446.

Boado, R.J., Li, J.Y., Nagaya, M., Zhang, C., Pardridge, W.M., 1999. Selective expression of the large neutral amino acid transporter at the blood–brain barrier. Proc. Natl. Acad. Sci. USA 96, 12079–12084.

Blondeau, J.P., Beslin, A., Chantoux, F., Francon, J., 1993. Triiodothyronine is a high-affinity inhibitor of amino acid transport system L1 in cultured astrocytes. J. Neurochem. 60, 1407–1413.

Chairoungdua, A., Segawa, H., Kim, J.Y., Miyamoto, K., Haga, H., Fukui, Y., Mizoguchi, K., Ito, H., Takeda, E., Endou, H., Kanai, Y., 1999. Identification of an amino acid transporter associated with the cystinuria-related type II membrane glycoprotein. J. Biol. Chem. 274, 28845–28848.

Christensen, H.N., Handlogten, M.E., Lam, L, Tager, H.S., Zand, R., 1969. A bicyclic amino acid to improve discriminations among transport systems. J. Biol. Chem. 244, 1510–1520.

Christensen, H.N., 1990. Role of amino acid transport and countertransport in nutrition and metabolism. Physiol. Rev. 70, 43–77.

Goldenberg, G.J., Lam, H.Y., Begleiter, A., 1979. Active carrier-mediated transport of melphalan by two separate amino acid transport systems in LPC-1 plasmacytoma cells in vitro. J. Biol. Chem. 254, 1057–1064.

Gomes, P., Soares-da-Silva, P., 1999. L-DOPA transport properties in an immortalized cell line of rat capillary cerebral endothelial cells, RBE 4. Brain Res. 829, 143–150.

Gravel, M., Gao, E., Hervouet-Zeiber, C., Parsons, V., Braun, P.E., 2000. Transcriptional regulation of 2',3'-cyclic nucleotide 3'-phosphodiesterase gene expression by cyclic AMP in C6 cells. J. Neurochem. 75, 1940–1950.

Kanai, Y., Segawa, H., Miyamoto, K., Uchino, H., Takeda, E., Endou, H., 1998. Expression cloning and characterization of a transporter for large neutral amino acids activated by the heavy chain of 4F2 antigen (CD98). J. Biol. Chem. 273, 23629–23632.

Kanai, Y., Endou, H., 2001. Heterodimeric amino acid transporters: molecular biology and pathological and pharmacological relevance. Curr. Drug Metab. 2, 339–354.

Kim, D.K., Kanai, Y., Chairoungdua, A., Matsuo, H., Cha, S.H., Endou, H., 2001. Expression cloning of a Na^+-independent aromatic amino acid transporter with structural similarity to H^+/monocarboxylate transporters. J. Biol. Chem. 276, 17221–17228.

Kim, D.K., Kanai, Y., Choi, H.W., Tangtrongsup, S., Chairoungdua, A., Babu, E., Tachampa, K., Anzai, N., Iribe, Y., Endou, H., 2002a. Characterization of the system L amino acid transporter in T24 human bladder carcinoma cells. Biochim. Biophys. Acta 1565, 112–121.

Kim, D.K., Kanai, Y., Matsuo, H., Kim, J.Y., Chairoungdua, A., Kobayashi, Y., Enomoto, A., Cha, S.H., Goya, T., Endou, H., 2002b. The human T-type amino acid transporter-1: characterization, gene organization, and chromosomal location. Genomics 79, 95–103.

Lakshmanan, M., Goncalves, E., Lessly, G., Foti, D., Robbins, J., 1990. The transport of thyroxine into mouse neuroblastoma cells, NB41A3: the effect of L-system amino acids. Endocrinology 126, 3245–3250.

Mannion, B.A., Kolesnikova, T.V., Lin, S.-H., Thompson, N.L., Hemler, M.E., 1998. The light chain of CD98 is identified as E16/TA1 protein. J. Biol. Chem. 273, 33127–33129.

Mastroberardino, L., Spindler, B., Pfeiffer, R., Skelly, P.J., Loffing, J., Shoemaker, C.B., Verrey, F., 1998. Amino-acid transport by heterodimers of 4F2hc/CD98 and members of a permease family. Nature 95, 288–291.

Matsuo, H., Tsukada, S., Nakata, T., Chairoungdua, A., Kim, D.K., Cha, S.H., Inatomi, J., Yorifuji, H., Fukuda, J., Endou, H., Kanai, Y., 2000. Expression of a system L neutral amino acid transporter at the blood–brain barrier. Neuroreport 11, 3507–3511.

McGivan, J.D., Pastor-Anglada, M., 1994. Regulatory and molecular aspects of mammalian amino acid transport. Biochem. J. 299, 321–334.

Nakamura, E., Sato, M., Yang, H., Miyagawa, F., Harasaki, M., Tomita, K., Matsuoka, S., Noma, A., Iwai, K., Minato, N., 1999. 4F2 (CD98) heavy chain is associated covalently with an amino acid transporter and controls intracellular trafficking and membrane topology of 4F2 heterodimer. J. Biol. Chem. 274, 3009–3016.

Oxender, D.L., Christensen, H.N., 1963. Evidence for two types of mediation of neutral amino acid transport in Ehrlich cells. Nature 197, 765–767.

Pfeiffer, R., Spindler, B., Loffing, J., Skelly, P.J., Shoemaker, C.B., Verrey, F., 1998. Functional heterodimeric amino acid transporters lacking cysteine residues involved in disulfide bond. FEBS Lett. 439, 157–162.

Pineda, M., Fernandez, E., Torrents, D., Estevez, R., Lopez, C., Camps, M., Lloberas, J., Zorzano, A., Palacin, M., 1999. Identification of a membrane protein, LAT-2, that Co-expresses with 4F2 heavy chain, an L-type amino acid transport activity with broad specificity for small and large zwitterionic amino acids. J. Biol. Chem. 274, 19738–19744.

Prasad, P.D., Wang, H., Huang, H., Kekuda, R., Rajan, D.P., Leibach, F.H., Ganapathy, V., 1999. Human LAT1, a subunit of system L amino acid transporter: molecular cloning and transport function. Biochem. Biophys. Res. Commun. 255, 283–288.

Rajan, D.P., Kekuda, R., Huang, W., Devoe, L.D., Leibach, F.H., Prasad, P.D., Ganapathy, V., 2000. Cloning and functional characterization of a Na^+-independent, broad-specific neutral amino acid transporter from mammalian intestine. Biochim. Biophys. Acta 1463, 6–14.

Rossier, G., Meier, C., Bauch, C., Summa, V., Sordat, B., Verrey, F., Kuhn, L.C., 1999. LAT2, a new basolateral 4F2hc/CD98-associated amino acid transporter of kidney and intestine. J. Biol. Chem. 274, 34948–34954.

Sang, J., Lim, Y.-P., Panzia, M., Finch, P., Thompson, N.L., 1995. TA1, a highly conserved oncofetal complementary DNA from rat hepatoma, encodes an integral membrane protein associated with liver development, carcinogenesis, and cell activation. Cancer Res. 55, 1152–1159.

Segawa, H., Fukasawa, Y., Miyamoto, K., Takeda, E., Endou, H., Kanai, Y., 1999. Identification and functional characterization of a Na^+-independent neutral amino acid transporter with broad substrate selectivity. J. Biol. Chem. 274, 19745–19751.

Sloan, J.L., Mager, S., 1999. Cloning and functional expression of a human Na^+ and Cl^--dependent neutral and cationic amino acid transporter $B^{0,+}$. J. Biol. Chem. 274, 23740–23745.

Su, T.Z., Lunney, E., Campbell, G., Oxender, D.L., 1995. Transport of gabapentin, a gamma-amino acid drug, by system I alpha-amino acid transporters: a comparative study in astrocytes, synaptosomes and CHO cells. J. Neurochem. 64, 2125–2131.

Tamai, S., Masuda, H., Ishii, Y., Suzuki, S., Kanai, Y., Endou, H., 2001. Expression of L-type amino acid transporter 1 in a rat model of liver

metastasis: positive correlation with tumor size. Cancer Detect Prev. 25, 439–445.

Uchino, H., Kanai, Y., Kim, D.K., Wempe, M.F., Chairoungdua, A., Morimoto, E., Anders, M.W., Endou, H., 2002. Transport of amino acid-related compounds mediated by L-type amino acid transporter 1 (LAT1): insights into the mechanisms of substrate recognition. Mol. Pharmacol. 61, 729–737.

Utsunomiya-Tate, N., Endou, H., Kanai, Y., 1996. Cloning and functional characterization of a system ASC-like Na^+-dependent neutral amino acid transporter. J. Biol. Chem. 271, 14883–14890.

Wilhelm, A., Volknandt, W., Langer, D., Nolte, C., Kettenmann, H., Zimmermann, H., 2004. Localization of SNARE proteins and secretory organelle proteins in astrocytes in vitro and in situ. Neurosci. Res. 48, 249–257.

Wolf, D.A., Wang, S., Panzia, M.A., Bassily, N.H., Thompson, N.L., 1996. Expression of a highly conserved oncofetal gene, TA1/E16, in human colon carcinoma and other primary cancers: homology to *Schistosoma mansoni* amino acid permease and *Caenorhabditis elegans* gene products. Cancer Res. 56, 5012–5022.

Yan, K., Popova, J.S., Moss, A., Shah, B., Rasenick, M.M., 2001. Tubulin stimulates adenylyl cyclase activity in C6 glioma cells by bypassing the beta-adrenergic receptor: a potential mechanism of G protein activation. J. Neurochem. 76, 182–190.

Yanagida, O., Kanai, Y., Chairoungdua, A., Kim, D.K., Segawa, H., Nii, T., Cha, S.H., Matsuo, H., Fukushima, J., Fukasawa, Y., Tani, Y., Taketani, Y., Uchino, H., Kim, J.Y., Inatomi, J., Okayasu, I., Miyamoto, K., Takeda, E., Goya, T., Endou, H., 2001. Human L-type amino acid transporter 1 (LAT1): characterization of function and expression in tumor cell lines. Biochim. Biophys. Acta 1514, 291–302.

Yoon, J.H., Kim, Y.B., Kim, M.S., Park, J.C., Kook, J.K., Jung, H.M., Kim, S.G., Yoo, H., Ko, Y.M., Lee, S.H., Kim, B.Y., Chun, H.S., Kanai, Y., Endou, H., Kim, D.K., 2004. Expression and functional characterization of the system L amino acid transporter in KB human oral epidermoid carcinoma cells. Cancer Lett. 205, 215–226.

Measurement of Glutamate Uptake and Reversed Transport by Rat Synaptosome Transporters

Atsushi NISHIDA,*[a] Hiroshi IWATA,[b] Yukitsuka KUDO,[c] Tsutomu KOBAYASHI,[a] Yuzo MATSUOKA,[a] Yoshikatsu KANAI,[d] and Hitoshi ENDOU[d]

[a] *Discovery and Pharmacology Research Laboratories, Tanabe Seiyaku Co., Ltd.; 2–2–50, Kawagishi, Toda, Saitama 335–8505, Japan:* [b] *Product Management Department, Pharmaceuticals Marketing Headquarters, Tanabe Seiyaku Co., Ltd.; 3–2–10, Dosho-machi, Chuo-ku, Osaka 541–8505, Japan:* [c] *Brain Function Research Institute, Inc., c/o National Cardiovascular Center; 5–7–1 Fujishiro-dai, Suita, Osaka 565–0873, Japan: and* [d] *Department of Pharmacology and Toxicology, Kyorin University School of Medicine; 6–20–2 Shinkawa, Mitaka, Tokyo 181–8611, Japan.*

Received November 27, 2003; accepted February 18, 2004

To establish an assay system for evaluation of the uptake and reversed transport of glutamate, we examined the effects of Na^+-concentration and pharmacological agents on the extracellular glutamate concentration ($[Glu]_o$) in rat cortical synaptosomes *in vitro*. There was a decrease and increase of the $[Glu]_o$ at high and low Na^+ concentrations, respectively, in a Ca^{2+}-free medium. The changes in $[Glu]_o$ in both directions were temperature-sensitive, and reversed at around 30 mM of Na^+. Dihydrokainate (DHK), a non-transportable inhibitor selective for glial glutamate transporter GLT-1, suppressed the decrease in $[Glu]_o$, and the reversal of $[Glu]_o$ change was shifted to about 60 mM Na^+. There was no change in the maximum $[Glu]_o$ at total Na^+ substitution. Further pharmacological analysis revealed that D-aspartate and DL-*threo*-β-hydroxy-aspartate (THA), transportable substrates of glutamate transporters, increased the $[Glu]_o$ in standard media. In contrast, β-phenylglutamic acid, a structural analogue of glutamate, suppressed both the decrease in $[Glu]_o$ in standard medium and the increase in $[Glu]_o$ in low Na^+ medium. It is, thus, concluded that both the direction and the amount of $[Glu]_o$ changes are determined by a balance of the uptake and reversed transport of glutamate, and that this assay system is suitable for evaluation of the effect of this on glutamate transporters.

Key words glutamate transporter; glutamate uptake; glutamate reversed transport; dihydrokainate; DL-*threo*-β-hydroxy-aspartate; synaptosome

The extracellular concentration of glutamate ($[Glu]_o$) is limited by the function of glutamate transporters located in both neuronal and glial membranes in the central nervous system.[1—8] Uptake of glutamate by these transporters is mediated by a secondary active transport process coupled with the transport of Na^+, K^+ and H^+.[1,6,9] Besides the exocytotic release upon depolarization of presynaptic terminals, glutamate can be released through transporters by "the reversed transport" process.[10—13] Reversed transport is induced by (1) an increase in cytoplasmic free substrates, (2) a decrease in the Na^+ electrochemical gradient, and (3) replacement of the intrinsic substrate in the synaptic vesicles by other transportable substrates.[12] Under ischemic conditions, $[Glu]_o$ is elevated to its neurotoxic levels due to the suppression of reuptake and to the reversed transport of glutamate upon the disrupted Na^+ gradient.[1,10—12]

The activity of glutamate transporters has been studied by measuring the uptake or release of radiolabelled glutamate in COS cells or *Xenopus* oocytes expressing glutamate transporters.[4,14] These heterologous expression systems are not suitable for studying reversed transport because these cell systems do not necessarily mimic conditions in the brain, such as the intracellular glutamate concentration, which affect the reversed transport. Furthermore, pre-existing glutamate often interferes with the transport of radiolabelled glutamate. In the present study, in order to evaluate the effects of drugs on both the forward and reversed transport of glutamate, we examined the effects of Na^+-concentration and pharmacological agents on external glutamate concentration in a rat cortical synaptosome preparation.

MATERIALS AND METHODS

Animals All experiments were performed under regulation of the Animal Ethics Committee of Tanabe Seiyaku Co., Ltd. Male Wistar strain rats weighing 200—400 g were used for the preparation of crude synaptosomal fractions.

Preparation of Crude Synaptosomal Fractions Crude synaptosomal fractions were prepared following the standard procedures.[15] Rats were anesthetized with ether, and whole brains were removed after decapitation. The cerebral cortex, isolated under an ice-cold condition, was homogenized in a 5-fold volume of 0.32 M sucrose. The homogenate was centrifuged at 1500×*g* for 10 min, and the supernatant was centrifuged at 9000×*g* for 20 min. The pellet (P2 fraction) was suspended in 0.32 M sucrose solution again and centrifuged at 9000×*g* for 20 min. The above procedures were carried out at 4 °C. The pellet was resuspended in 0.32 M sucrose, then used as a crude synaptosome preparation in the following experiments. The protein content of the crude synaptosome preparation was 6.78±0.11 mg/ml (mean±S.E., n=37). The glutamate content in the synaptosomal preparation is of intrinsic origin.

Determination of Extracellular Glutamate in Synaptosomal Preparation Fifty microliters of the crude synaptosome preparation was added to 1 ml of standard HEPES buffered saline (HBS) medium containing 140 mM NaCl, 5 mM KCl, 5 mM $NaHCO_3$, 1 mM $MgCl_2$, 0.12 mM Na_2SO_4, 10 mM glucose, and 20 mM HEPES (pH 7.4) on ice with or without drug. In order to evoke the glutamaterelease by depolarization, we prepared a high-K solution by adding 20 μl of 4 M KCl and 1 μl of 2 M $CaCl_2$ into HBS medium. The reaction was started by transferring the incubation tube into a

* To whom correspondence should be addressed. e-mail: bon@tanabe.co.jp

37 °C water bath. The ice-cold medium reached 37 °C in 60 to 70 s. After incubation at 37 °C for up to 6 min, except for the experiments in Fig. 1, the reaction was stopped by immediately transferring the incubation tube into an ice-cold water bath. It took 70 to 80 s to reach 10 °C or less from 37 °C. Then, the synaptosomes were centrifuged at 9000×*g* for 20 min at 4 °C, and the supernatants were stocked at −80 °C until the measurement of glutamate. The concentration of glutamate in the supernatants was determined using the glutamate dehydrogenase-NADP$^+$ method.[16] The difference in glutamate concentration in each media before and after incubation was expressed as $\Delta[Glu]_o$ (μM) {([Glu]$_o$ after incubation)−([Glu]$_o$ before incubation)}. "Positive" values of $\Delta[Glu]_o$ represent an increase in glutamate outside synaptosomes, whereas "negative" values represent a decrease in glutamate outside synaptosomes.

Chemicals The following materials were of reagent grade and obtained from commercial sources: sucrose, choline chloride, HEPES (Nacalai Tesque Co. Ltd, Tokyo); DL-*threo*-β-hydroxy-aspartate (THA), dihydrokainate (DHK), (±)-β-phenylglutamic acid, (±)-β-*p*-chlorophenyl-glutamate (Tocris Cookson, Inc., St. Louis, MO, U.S.A.); L-carnitine, D-aspartate, baclofen, glutamate dehydrogenase and NADP (Sigma Chemicals Co. Ltd., St. Louis).

RESULTS

Incubation of synaptosomes for 10 min with 80 mM K^+ significantly increased [Glu]$_o$ in the presence of 2 mM Ca^{2+} (Fig. 1). Substitution of NaCl with choline chloride ([Na^+]$_o$=5.24 mM) also increased [Glu]$_o$, even in the Ca^{2+}-free condition. The latter increase was not observed at a low temperature when the synaptosomes were kept on ice.

When synaptosomes were incubated at 37 °C in the standard HBS medium, [Glu]$_o$ was decreased upon incubation (Fig. 2). The [Glu]$_o$ value at time 0 was 4.53±0.41 μM. The maximal reduction was achieved within 2 min, and the level of [Glu]$_o$ was maintained up to 6 min. When synaptosomes were incubated in a low Na^+ medium in which NaCl was substituted with choline chlolide ([Na^+]$_o$=5.24 mM), there was a prompt increase in [Glu]$_o$. The [Glu]$_o$ value at time 0 was 5.17±0.51 μM. The maximal increase was achieved within 4 min.

Reduction of Na^+ by substitution with choline to about 60 mM from 145.2 mM did not affect the $\Delta[Glu]_o$. However, when Na^+ was reduced to about 30 mM, there was no change in $\Delta[Glu]_o$. $\Delta[Glu]_o$ was markedly increased upon further replacement of Na^+ with choline (Fig. 3).

D-Aspartate, a transportable inhibitor of excitatory amino acid transporters (EAATs),[2,11,17] rapidly increased [Glu]$_o$ in standard HBS medium ([Na^+]$_o$=145.2 mM) and failed to inhibit the increase in [Glu]$_o$ in the low Na^+ medium ([Na^+]$_o$= 5.24 mM) (Fig. 4). The increase in [Glu]$_o$ by D-aspartate in a standard HBS medium was comparable to that in the low Na^+ medium.

DHK, a non-transportable inhibitor of glilal glutamate transporter (GLT-1), inhibited the reduction of [Glu]$_o$ in a standard HBS medium, and upwardly shifted the

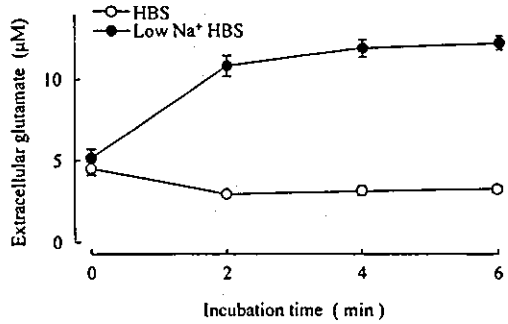

Fig. 2. Time Course of Uptake and Reversed Transport of Glutamate *via* Rat Synaptosomal Glutamate Transporters

Synaptosomes were incubated at 37 °C in the standard HBS medium or the medium in which Na^+ was replaced by choline from 145.2 mM to 5.24 mM. Each point represents the mean±S.E. of 5 experiments.

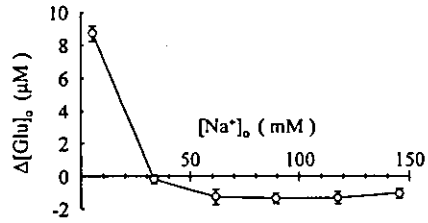

Fig. 3. Effects of Na^+ Concentration on $\Delta[Glu]_o$

Synaptosomes were incubated for 6 min at 37 °C in the medium with various Na^+ concentrations. Each point represents the mean±S.E. of 5 experiments. $\Delta[Glu]_o$ was reversed from negative to positive values at about 30 mM Na^+ by substitution of choline.

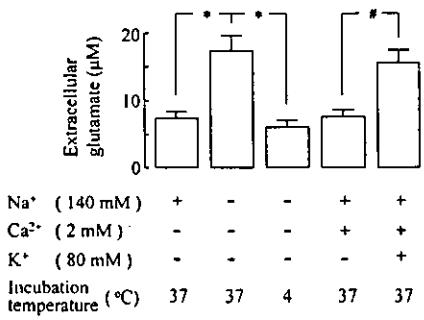

Fig. 1. Glutamate Release by Exocytosis and Reversed Transport in Rat Cerebral Cortical Synaptosomes

Reversed transport was induced by the substitution of NaCl in the standard HBS medium with choline chloride. Each column represents the mean±S.E. of 6 experiments. *p<0.01 compared to the second left column by randomized block design, followed by the Bonferroni method. #p<0.001 compared to the second right column by paired t-test.

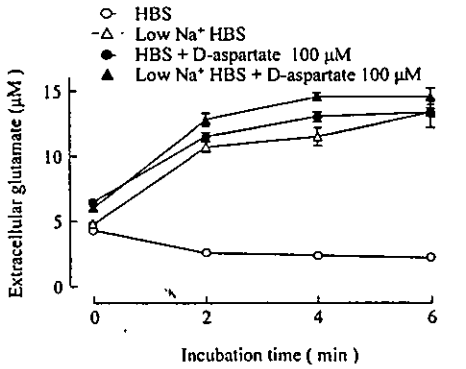

Fig. 4. Effects of D-Aspartate on the Uptake and Reversed Transport of Glutamate *via* Rat Synaptosomal Glutamate Transporters

Synaptosomes were incubated at 37 °C in the standard HBS or low Na^+ HBS medium ([Na^+]$_o$=5.24 mM) in the presence or absence of D-aspartate. Each point represents the mean±S.E. of 4 experiments.

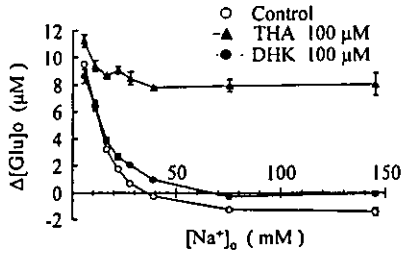

Fig. 5. Effects of DHK and THA on $\Delta[Glu]_o$

Synaptosomes were incubated for 6 min at 37 °C in the medium with various Na^+ concentrations. Na^+ was substituted with choline. Each point represents the mean±S.E. of 4 experiments.

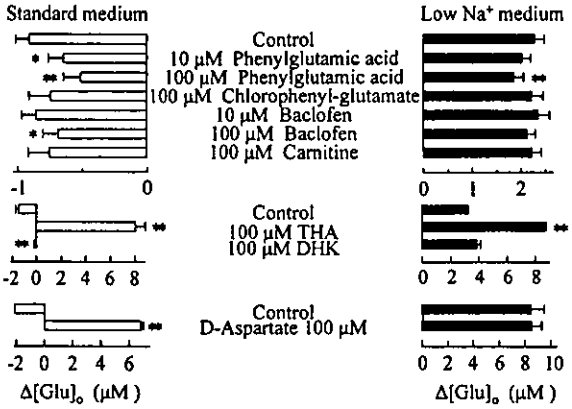

Fig. 6. Effects of (±)-β-Phenylglutamic Acid, (±)-β-*p*-Chlorophenyl-glutamate, Baclofen and L-Carnitine on $\Delta[Glu]_o$ in Standard HBS Medium and Low Na^+ Medium

Each column represents the mean±S.E. of 5 experiments. $*p<0.05$, $**p<0.01$ *vs.* control, comparison by one-way ANOVA with randomized complete block, followed by multiple comparison (Dunnett's method). Effects of THA, DHK and D-aspartate were reconstructed from Fig. 4 and Fig. 5 for reference. Low Na^+ medium ($[Na^+]_o$=16.4 mM) was prepared from standard HBS medium ($[Na^+]_o$=145.2 mM) by substitution of Na^+ with choline, except for the evaluation of aspartate. $**p<0.01$ *vs.* control, comparison by Student's *t*-test.

$[Na^+]_o-\Delta[Glu]_o$ curve (Fig. 5). In contrast, THA, a transportable inhibitor, caused a marked increase in $[Glu]_o$, even in standard HBS medium.

Next, we examined the effects of several glutamate analogues on $\Delta[Glu]_o$. (±)-β-Phenylglutamic acid inhibited both the decrease in $[Glu]_o$ observed in the standard HBS medium and the increase in $[Glu]_o$ in a low Na^+ medium ($[Na^+]_o$=16.4 mM) (Fig. 6). Baclofen, a $GABA_B$ receptor agonist, also significantly suppressed the decrease of $[Glu]_o$ in the standard HBS medium. (±)-β-*p*-Chlorophenyl-glutamate and carnitine at 100 μM affected neither the $[Glu]_o$ in standard HBS medium nor that in the low Na^+ medium.

DISCUSSION

Glutamate is co-transported with Na^+ and H^+ and counter-transported with K^+ *via* glutamate transporters.[6,9,18] Because forward and reversed transport of glutamate is affected by the concentration gradients of these ions across plasma membrane as well as the membrane potential, we examined the effect of external Na^+ concentration on glutamate transport in the synaptosome preparation. Synaptosomes were prepared from a homogenate of rat cerebral cortex. Due to leaking of glutamate from cells by this operation, the glutamate concentration outside of synaptosomes in this study was higher than that under physiological condition. The higher the glutamate concentration, the more pronounced the driving force of uptake. Thus, the influence of various treatments on the uptake system using synaptosomes can be easily detected.

In the present study, we showed that $[Glu]_o$ in the synaptosome preparations was changed depending on temperature and Na^+ concentration of the incubation medium. Glutamate was taken up by synaptosomes at a physiological concentration of extracellular Na^+, whereas at low Na^+ concentration, the synaptosomes released glutamate into the incubation medium. $\Delta[Glu]_o$ was reversed from negative to positive at about 30 mM $[Na^+]_o$. The changes in glutamate, $\Delta[Glu]_o$, appear to indicate a balance between the amount of uptake and reversed transport by transporters. Intracellular glutamate may be released to an extracellular site *via* glutamate transporters at this ion-coupling stoichiometry.[18]

DHK, a non-transportable inhibitor selective for GLT-1,[21,22] upwardly shifted the $[Na^+]_o-\Delta[Glu]_o$ curve (Fig. 5). The area surrounded by two curves in the presence and absence of DHK is supposed to represent the uptake of glutamate into the glial component by DHK-sensitive GLT-1. The area under the curve for DHK and over the x axis may represent the reversed transport *via* DHK-insensitive glutamate transporters, such as EAAC1. The synaptosome fraction consists of both glial and neuronal components.[23] The intracellular glutamate concentrations are 50 μM and 1 mM for glia and neurons, respectively.[24] Because of the high concentration of glutamate in neurons, the conversion of uptake/reversed uptake in neurons takes place at a higher extracellular Na^+ concentration than in the glia. While the neuronal glutamate transporters are functionally converted from an uptake-predominant to a release-predominant state by a reduction in Na^+ from 145.2 mM to about 60 mM, the uptake of glutamate by glial GLT-1 is maintained. GLT-1 may contribute to the uptake rather than the reversed transport in this assay system. In the low Na^+ condition, DHK slightly increased but did not decrease $[Glu]_o$, and thus, it is presumed to be a typical uptake inhibitor without any effect on the reversed transport.

Glutamate transporters mediate not only substrate uptake and reversed transport but also the heteroexchange of substrates in a Na^+ dependent manner.[20] The uptake of [^{3}H]-glutamate into synaptosomes is inhibited by D-aspartate and THA.[6,19] In the present study, both D-aspartate and THA extensively increased the $[Glu]_o$ in the standard HBS medium, most likely mediated by a heteroexchange of the substrates. As shown above, the glutamate uptake by GLT-1 is maintained at 16.4 mM $[Na^+]_o$, and is functionally converted to the release-predominant state at about 10 mM $[Na^+]_o$. In accord, THA increased $[Glu]_o$ at 16.4 mM $[Na^+]_o$, but D-aspartate did not affect the $[Glu]_o$ at 5.24 mM $[Na^+]_o$. Thus, the heteroexchange of glutamate is properly evaluated in this assay system.

Extracellular glutamate plays a fundamental role in ischemic brain damage. The $[Glu]_o$ in the ischemic brain is increased either by exocytotic release or reversed transport of glutamate from glutamate-containing neurons.[10–13] Because the drugs inhibiting $[Glu]_o$ elevation have a potential for preventing ischemic brain damage,[25] we analyzed the effect of some glutamate-related compounds on $[Glu]_o$ in this assay system. Among the glutamate analogs tested, (±)-β-phenyl-

glutamic acid significantly suppressed both the elevation of $[Glu]_o$ in low Na^+ medium and the reduction of $[Glu]_o$ in standard HBS medium. This compound is, thus, proposed to inhibit both uptake by glial transporters and reversed transport by neural transporters. This beneficial action of (±)-β-phenylglutamic acid, to our knowledge, has not been reported. The potential of this compound to suppress ischemia-induced brain damage is to be examined.

Previously, the transport of glutamate has been characterized using radiolabelled glutamate in COS cells or in *Xenopus* oocytes expressing glutamate transporters.[4,14] There was, however, a limitation of these heterologous expression systems to analyze the glutamate release because these cell systems do not necessarily mimic conditions in brain, such as intracellular glutamate concentration, which affects the reversed transport. Furthermore, possible interference of the transport of labeled glutamate by pre-existing glutamate cannot be excluded. The measurement of $[Glu]_o$ has several advantages over the previous methods, as follows: (1) extracellular glutamate is determined without using radiolabelled compounds, (2) the synaptosome preparations (P2 fraction) contain both neuronal and glial components, including intrinsic glutamate, and (3) transportable and non-transportable inhibitors can be distinguished.

In conclusion, we developed an *in vitro* assay system to evaluate the effect of drugs on the uptake and reversed transport of glutamate in synaptosomes. Because extracellularly released glutamate plays a crucial role in ischemic brain damage, this assay system would be useful for the evaluation of neuroprotective agents that affect glutamate transporters.

Acknowledgments We thank Dr. Akira Saito for valuable discussions during the preparation of this article.

REFERENCES

1) Bouvier M., Szatkowski M., Amato A., Attwell D., *Nature* (London), **360**, 471—474 (1992).
2) Kanai Y., Hediger M. A., *Nature* (London), **360**, 467—471 (1992).
3) Kanai Y., Smith C. P., Hediger M. A., *Trends Neurosci.*, **16**, 365—370 (1993).
4) Kawakami H., Tanaka K., Nakayama T., Inoue K., Nakamura S., *Biochem. Biophys. Res. Commun.*, **199**, 171—176 (1994).
5) Pines G., Danbolt N. C., Bjoras M., Zhang Y., Bendahan A., Eide L., Koepsell H., Storm-Mathisen J., Seeberg E., Kanner B. I., *Nature* (London), **360**, 464—467 (1992).
6) Robinson M. B., Hunter-Ensor M., Sinor J., *Brain Res.*, **544**, 196—202 (1991).
7) Tanaka K., *Neurosci. Res.*, **16**, 149—153 (1993).
8) Tanaka K., *Neurosci. Lett.*, **159**, 183—186 (1993).
9) Kanai Y., Nussberger S., Romero M. F., Boron W. F., Hebert S. C., Hediger M. A., *J. Biol. Chem.*, **270**, 16561—16568 (1995).
10) Attwell D., Barbour B., Szatkowski M., *Neuron*, **11**, 401—407 (1993).
11) Kanai Y., Stelzner M., Nussberger S., Khawaja S., Hebert S. C., Smith C. P., Hediger M. A., *J. Biol. Chem.*, **269**, 20599—20606 (1994).
12) Levi G., Raiteri M., *Trends Neurosci.*, **16**, 415—419 (1993).
13) Szatkowski M., Attwell D., *Trends Neurosci.*, **17**, 359—365 (1993).
14) Shimada F., Shiga Y., Morikawa M., Kawazura H., Morikawa O., Matsuoka T., Nishizaki T., Saito N., *Eur. J. Pharmacol.*, **386**, 263—270 (1999).
15) Hajos F., *Brain Res.*, **93**, 485—489 (1975).
16) Graham L. T., Jr., Aprison M. H., *Anal. Biochem.*, **15**, 487—497 (1966).
17) Wadiche J. I., Amara S. G., Kavanaugh M. P., *Neuron*, **15**, 721—728 (1995).
18) Zerangue N., Kavanaugh M. P., *Nature* (London), **383**, 634—637 (1996).
19) Garlin A. B., Sinor A. D., Sinor J. D., Jee S. H., Grinspan J. B., Robinson M. B., *J. Neurochem.*, **64**, 2572—2580 (1995).
20) Zerangue N., Kavanaugh M. P., *J. Physiol.* (London), **493**, 419—423 (1996).
21) Chatton J. Y., Shimamoto K., Magistretti P. J., *Brain Res.*, **893**, 46—52 (2001).
22) Kanai Y., *Curr. Opin. Cell Biol.*, **9**, 565—572 (1997).
23) Danbolt N. C., Storm-Mathisen J., Kanner B. I., *Neuroscience*, **51**, 295—310 (1992).
24) Kanai Y., Smith C. P., Hediger M. A., *FASEB J.*, **7**, 1450—1459 (1993).
25) Yamashita H., Kawakami H., Zhang Y., Tanaka K., Nakamura S., *Lancet*, **346**, 1305 (1995).